THE EVOLUTION AND STRATIGRAPHIC ARCHITECTURE OF FLUVIO-LACUSTRINE DELTAS: RESERVOIR CHARACTERISTICS FROM THE RED RIVER DELTA, LAKE TEXOMA AND THE DENTON CREEK DELTA, GRAPEVINE LAKE, TX

by

TYLER HOWE

Bachelor of Science, Geology, 2015

University of Oklahoma

Norman, Oklahoma

Submitted to the Graduate Faculty of the

College of Science and Engineering

Texas Christian University

in partial fulfillment of the requirements

for the degree of

Master of Science, Geology

May 2017

ACKNOWLEDGEMENTS

The work represented herein is a culmination of the support I have received from many people throughout the last two years.

I would like to thank my father Todd and my brother Tanner for being my dependable data collection team and weathering a few storms at Lake Texoma and Grapevine Lake. Without your help, this work would not be what it is.

I want to thank my fiancé, Sheena, for her kind understanding and help in keeping me grounded throughout this work.

Thank you to Woodside Petroleum for funding part of this research. I truly appreciate the support from across the pond.

I offer my sincerest gratitude to Dr. John Holbrook for taking me on as his student, trusting me with his ideas in the form of this project, and for his exceptional guidance to see it through.

TABLE OF CONTENTS

LIST OF FIGURES

CHAPTER 1 - INTRODUCTION

This research details the sedimentary deposits of two modern lacustrine deltas: the Red River Delta in Lake Texoma, and the Denton Creek Delta in Grapevine Lake. The word delta was first used to describe a geological body by the Greek historian Herodotus (484-425 BC), who noted the similarity between the Nile River mouth deposits and the triangular symbol for the Greek letter delta (Celoria, 1966). Deltas have the potential to fill all laterally available basin space with sediment through multiple bifurcation events from its apex, forming a deposit with lobate "delta" geometry. The expectation that lobate deltas are the de-facto landform created when a river meets an open body of water, however, has long been modified (e.g. Galloway, 1975). This study in fact questions if deltas must bifurcate at all. Single-channel, progradational, non-bifurcating deltas are currently forming in many man-made lakes throughout the United States. This study will investigate the sedimentary facies and architecture currently forming in two of these elongate, fluvial-dominated lacustrine deltas and propose a model for their formation. An increased understanding of the facies created by single-channel lacustrine deltas and the aspect ratios of the associated architectural elements they produce will improve predictive reservoir models for fluvio-lacustrine environments.

Rivers that carry a higher median grain size are more likely to form mouth bars, which drive bifurcation of flow, resulting in a more lobate delta morphology (Edmonds and Slingerland, 2010; Caldwell, 2013). These same studies conversely show mud dominated deltas bifurcate much less due to a lack of sand in the river mouth. Surprisingly, work by Tomanka (2013) showed that the mixed-load Denton Creek delta in Grapevine Lake did not bifurcate at all. Presumably a more sandy, bedload dominated river should easily form sandy mouth bars that drive bifurcation. However, the Red River Delta at Lake Texoma is enigmatic in this way; it is a

sandy, bedload dominated river with a 2ϕ median bedload grain size (Schwartz, 1978) that forms an elongate, non-bifurcating delta. The Red River also forms a permanent hyperpycnal flow into Lake Texoma due to the higher river water density relative to the lake basin (Olariu et al., 2012). Hyperpycnal flows, due to increased friction between the jet and the basin floor, are more likely to form mouth bars as opposed to significant levee deposits, further driving bifurcation (Bates, 1953).

Previous work on the Red River Delta proposed that the morphology is controlled by a combination of fluvial discharge and basin bathymetry (Olariu et al., 2012). In this model, during times of high discharge, the delta would respond to the increased flow inertia and straighten its course; during periods of low discharge, the delta would switch to a lobate geometry and fill all laterally available basin space (Olariu et al., 2012). Here we offer a different hypothesis for the morphology of the Red River Delta.

The Red River Delta should form a lobate delta based on its high median grain size combined with its hyperpycnal flow into Lake Texoma. We hypothesize that the elongate, single-channel morphology that forms instead could be due the sand in the system simply not reaching the river mouth where the delta is built. The lack of sand at the mouth of the Red River may be due to a process of grain size segregation within the Red River channel that is similar to what Hull (2016) found in tie channels of the Grijalva River system. If the Red River Delta is forming in accordance with his “gun-barrel” model for propogating channels, then we should find an absence of sand at the mouth of the river and sand sheets forming as overbank flood deposits similar to the “wings” described in Tomanka (2013).

1.1. Controls on delta morphology

Deltas form when a river carrying sediment terminates flow into a basin and gradient is lost. The hydrodynamic energy transfer from the flow of the river into a quiescent basin results in the deposition of sediment near the mouth of the river. The relative energy between the river and the receiving basin influences the geometry of the deltaic deposit. These include aspects of the fluvial system such as flow velocity, channel aspect ratio, and flood periodicity, which interact with basinal characteristics such as water depth and the processes of waves and tides (Wright & Coleman, 1973; Postma, 1990).

1.1.1. Turbulent jet theory

Research in the field of hydrodynamics offered initial insights into river mouth processes. Turbulent jet theory was described by Tollmien in 1926 (Bates, 1953), and expanded upon by several others (Abramovich, 1963; Wright, 1977; Hoyal, 2003). A turbulent jet occurs when a flowing fluid enters a still body of water, creating a spreading fluid plume. Aspects of the jet include a map-view Gaussian velocity profile at the front of the plume (Fig. 1) with flow rate initially decreasing at the centerline four orifice distances out, and mixing of jet and basin fluid at the jet margins (Hoyal, 2003). Sediment distributed within a jet is subject to the same marginal mixing as the fluid. Particle flow paths are controlled by the velocity field of the jet, therefore the jet controls river mouth sedimentation patterns. Subaqueous levees form at the margins of the jet and river mouth bars form under the center of the jet (Fagherazzi et al., 2015).

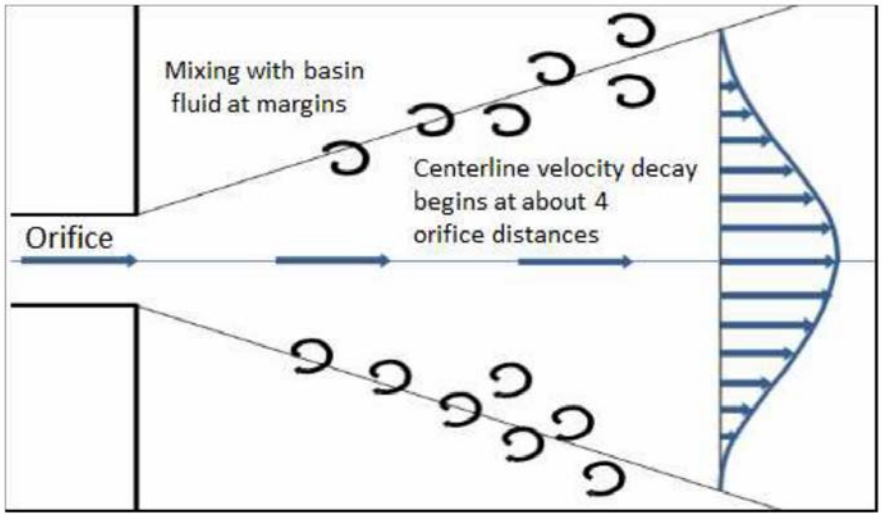

Fig. 1: Turbulent jet spreading model. Main features are the Gaussian velocity profile of a spreading plume, mixing of sediment along the margins forming levees, and centerline velocity decay. From Boggs (1995), modified from Bates (1953).

Jet theory was expanded on by Bates (1953) to account for density differences between the fluids in the river and the basin, producing the concepts of homopycnal, hypopycnal, and hyperpycnal flows (Fig. 2). Homopycnal flow occurs when river inflow is of equal density with the basin water, resulting in a plume that deposits sediment equally in the water column. Hypopycnal flow occurs when river inflow is less dense than the basin water, resulting in a plume that flows as suspension on top of the basin water and deposits sediment through flocculation. Hyperpycnal flow occurs when the river flow has a higher density than the basin, resulting in a bed contact flow that deposits sediment along the basin floor.

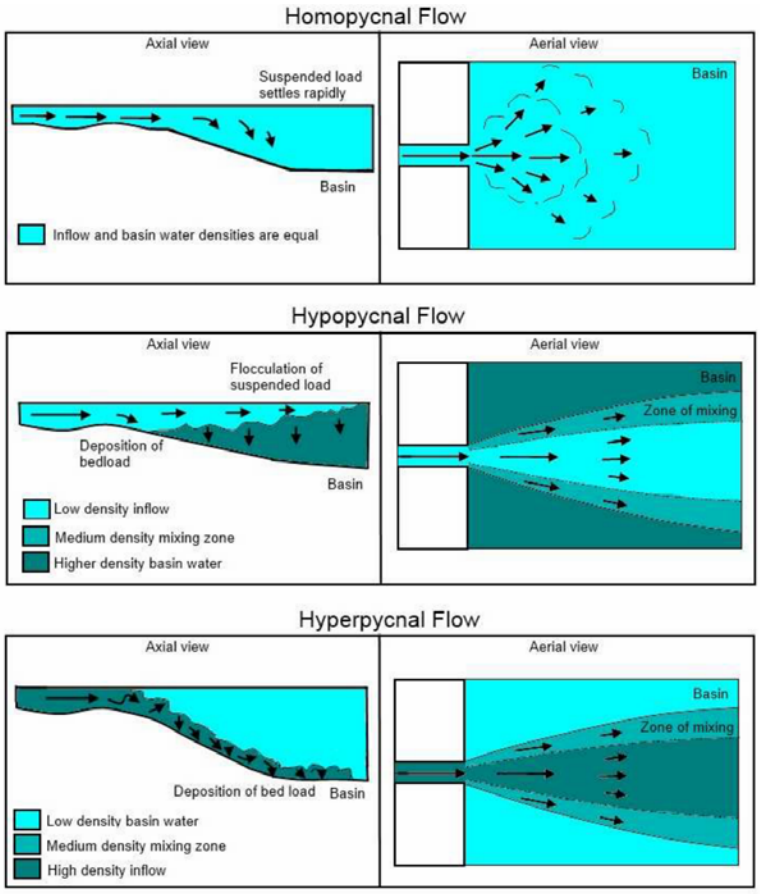

Fig. 2: Flow regimes for water entering a basin based on the relative density of the inflow and basin fluid density. The Red River delta is forming as a hyperpycnal flow. Figure from Boggs (1995), modified after Bates (1953).

Wright (1977) was the first to link conditions of the turbulent jet to delta morphology. Wright suggested that delta morphology is influenced by the relative intensities of outflow inertia, bed friction, and buoyancy. According to his model, outflow inertia dominance from homopycnal flow is characterized by an unrestricted turbulent jet spreading into a deep basin, which produces lunate bars and short deltas with high accretion angles known as Gilbert deltas. Bed friction dominance from hyperpycnal flow leads to rapid plume spreading and sediment divergence around mouth bar deposits, leading to more bifurcations and terminal distributary channels, forming lobate deltas. Buoyancy dominance from hypopycnal flow produces parallel banks, high depth-to-width ratios, and low bifurcation frequency, forming elongate deltas.

According to Galloway (1975), basin currents overprint depositional trends inherent from the river jet and variations in the proportions of river, wave, and tidal energy are the primary factors influencing delta morphology (Fig. 3). In his model, intense river discharge promotes progradation into the basin, producing elongated deltas such as the modern birdsfoot lobe of the Mississippi River. Tidal currents rework sediment perpendicular to the shoreline, resulting in multiple distributary channels separated by parallel bars. Wave surge distributes sediment along the shoreline and creates wide lobate deltas. Galloway's tertiary classification captures some of the main controls on delta morphology; however, it is commonly used as an oversimplification of the complex interplay of processes that form deltas due to the tendency to categorize mixed influence deltas as one of the three end members, as pointed out by Bhattacharya & Giosan (2003).

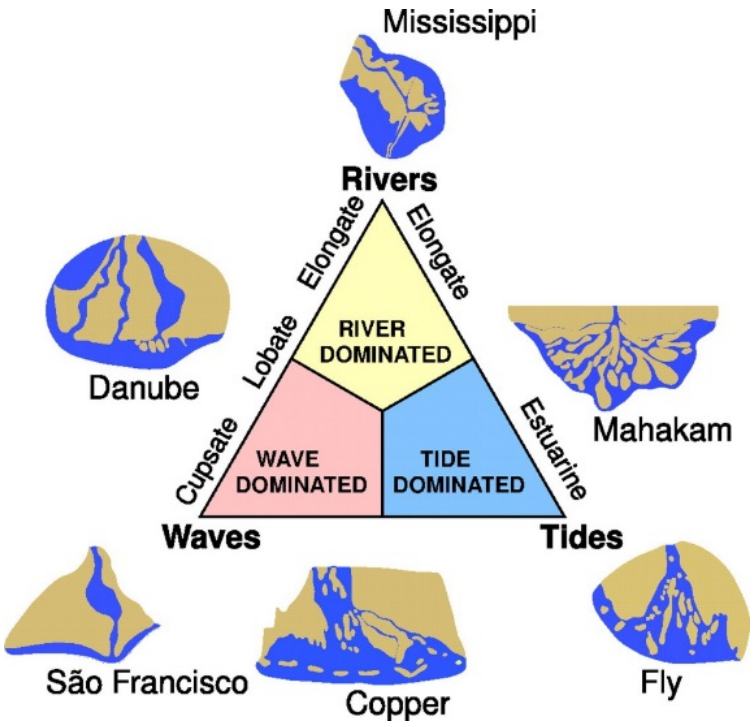

Fig. 3: Triangular classification of deltaic depositional systems. Modified after Galloway, 1975.

1.1.2. Jet impact on mouth bar and subaqueous levee deposition

A turbulent jet can be divided into two zones based on different flow behavior: the zone of flow establishment (ZOFE) and the zone of established flow (ZOEF) (Fig. 4) (Ozsoy and Unluata, 1982). The ZOFE is near the river mouth, and is characterized by a constant centerline velocity. The ZOEF begins when the turbulence generated by the shear stress at the jet margins affects the entire jet flow. The location of the transition from the ZOFE to the ZOEF is critical because it is associated with the threshold loss in flow competency that causes the deposition of mouth bars (Bates, 1953).

Predicting the distance from the river mouth that the mouth bar will form can be tested experimentally. Original flume experiments studying turbulent jets were done in an "unbounded" fluid environment, with a sufficiently large water tank to not interfere with the jet. The flow competence was found to decline at a distance of 0 to 6 river mouth orifices out (Albertson et al., 1950; Tennekes & Lumley, 1972, Edmonds and Slingerland, 2007). More recently, researchers have switched to using "bounded" or shallow jets, which better represent a river mouth by incorporating both free turbulence and wall shear turbulence (Fig. 4) (Jirka, 1994). Flume experiments of bounded jets reveal that mouth bar deposition initiated by the transition from the ZOFE to ZOEF occurs at a distance into the basin of 16 to 18 river mouth orifices (Rowland, 2009a). The shallow, bounded jet forms mouth bars further out due to increased lateral diffusion of sediment that enhances levee formation by removing sediment from the jet centerline (Canestrelli et al., 2014).

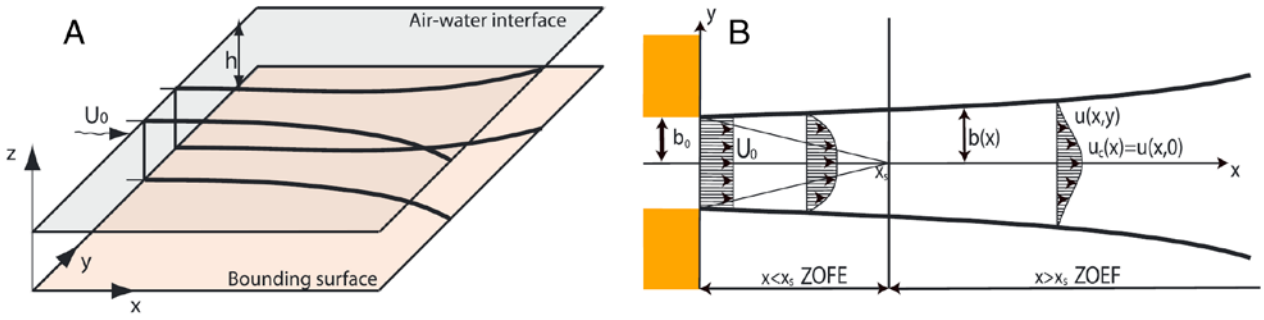

Fig. 4: (A) Diagram of a plane bounded, shallow jet, which better represents a river mouth by incorporating both free turbulence and wall shear turbulence (Canestrelli et al., 2014). (B) Diagram of a turbulent jet showing the zone of flow establishment (ZOFE) and the zone of established flow (ZOEF) (Nardin et al., 2013).

Once the location of a mouth bar is set, there is a general pattern of deposition from initial bar formation to distributary bifurcation. The four stages of mouth bar deposition are (Fig. 5) (Edmonds and Slingerland, 2010):

(1) Subaqueous levees form parallel to the channel coinciding with the formation of a small mouth bar (Fig 5A).

(2) Subaqueous levees extend linearly and the mouth bar progrades basinward and aggrades (Fig 5B).

(3) Mouth bar deposition ceases and the subaqueous levees flare outward around the mouth bar (Fig 5C).

(4) The river mouth bar breaches the water surface and the primary river channel bisects into two distributary channels, one on each side of the mouth bar.

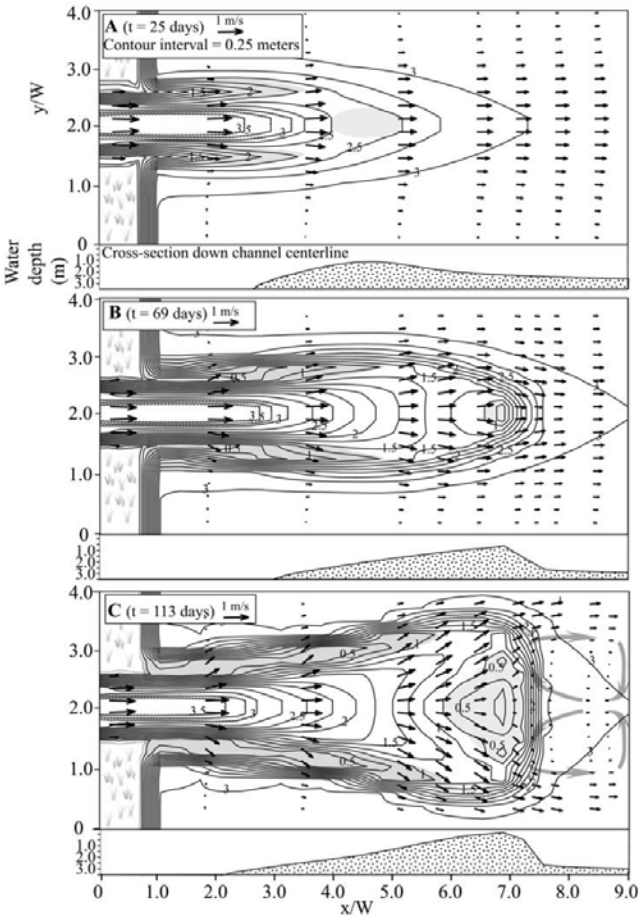

Fig. 5: Contour maps created from Delft3D simulation depicting stages mouth bar deposition. (A) Early mouth bar deposition with straight levees. (B) Mouth bar progrades and aggrades as levees extend. (C) Mouth bar aggrades sufficiently to split flow as levees flare, inducing bifurcation of the channel (from Edmonds and Slingerland, 2007).

Grain size is also linked to delta morphology (Orton and Reading, 1993; Hoyal and Sheets, 2009; Edmonds and Slingerland, 2010). Orton and Reading (1993) (Fig. 6) suggested that grain size was the fourth control along with Galloway's (1975) tertiary model for river, wave, and tidal influence (Fig. 3). Numerical modeling indicates that grain size impacts delta development due to smaller grain sizes having higher cohesion (Edmonds and Slingerland, 2010; Caldwell and Edmonds, 2014). Cohesion of the sediment within the river was found to affect the river mouth depth-to-width ratio, which alters the turbulent jet and influences the delta to be

more elongated. Essentially, when all other factors are held constant, rivers with a coarser median grain size are more likely to create mouth bars, leading to increased bifurcation frequency, increased distributary channel formation, and ultimately a more lobate planform geometry (Caldwell, 2013).

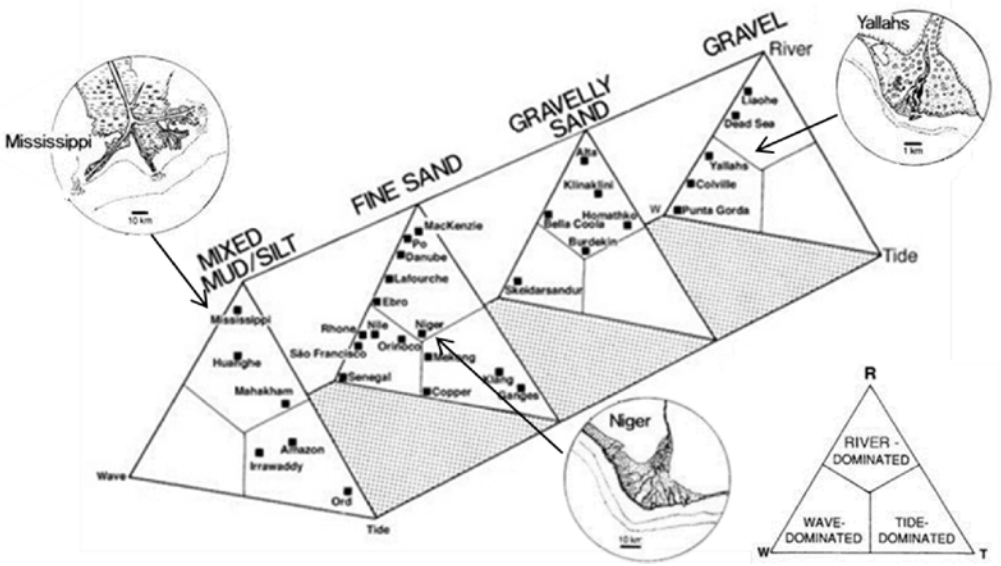

Fig. 6: Grain size can be thought of as the 4th control on delta morphology after river, wave, and tidal energy (From Caldwell 2013, modified from Orton and Reading, 1993).

Recent research on the effects that river mouth processes have on mouth bar and levee deposition has extended from the qualitative to the quantitative realm. Numerical models that couple hydrodynamic and sediment transport equations allow long time scales of deltaic deposition to be studied (e.g. Overeem et al. 2005, Fagherazzi and Overeem, 2007). These models are especially useful to investigate the effect of one variable by keeping all others constant. High-resolution flumes are also used to observe relationships between turbulent jet hydrodynamics and sediment transport (Rowland et al., 2009). These quantitative approaches are useful for elucidating the potential controls on delta morphology. Field-based sedimentological

studies of deltas (e.g. Tomanka, 2013; Esposito et. al., 2013; Hull, 2016) are increasingly important to compare with and assess these numerical and lab-based models.

Since Wright's 1977 synthesis, significant work has been done to expand our understanding of the effects and relative influence that waves (e.g. Bhattacharya and Giosan, 2003; Jerolmack and Swenson, 2007; Ashton and Giosan, 2011; Nardin and Fagherazzi, 2012; Nardin et al., 2013) and tides (e.g. Dalrymple and Choi, 2007; Fagherazzi, 2008; Leonardi et al., 2013) have on deltaic morphology, facies, and architecture. However, waves and tides are basinal conditions that alter the fluvial jet, usually in a dispersive manner that promotes bifurcation. In order to understand default deltaic deposition, river mouth processes may be studied in the absence of these dispersive processes. The hydrodynamics and depositional patterns at river outlets are set in place by the river jet; therefore, the fluvial system can be thought of, and studied, as the first order deltaic control.

1.1.3. Fluvial-dominated elongate deltas

The linear end member of Galloway's (1975) triangular classification of deltas is the river-dominated delta; these deltas are thought to have a morphology determined predominantly by the energy of the river. The most commonly cited example of this end member is the Balize or "birdsfoot" lobe of the Mississippi River Delta (Fig. 7). The cause of the Mississippi Delta morphology is widely investigated (e.g. Bates, 1953; Galloway, 1975). Some authors attribute the modern birdsfoot morphology to high sediment cohesion leading to resistant levees inhibiting avulsion and breakdown of mouth bars (Edmonds, 2009), while some attribute it to the interplay between maximum monthly discharge and the low degree of marine influence (Syvitski and

Saito, 2007). Notable characteristics of the birdsfoot lobe are its elongated shape, high length-to-width ratio, and low bifurcation rate. Although the birdsfoot lobe is an example of an elongated delta, there are other fluvial-dominated deltas that bifurcate at an even lower rate.

Fig. 7: The modern birdsfoot lobe of the Mississippi Delta is a common example of a fluvial-dominated delta, where the elongated morphology is influenced by the discharge from the river system (image courtesy NASA Visible Earth)

A system that can form a linear channel into a basin without bifurcation is a tie channel. First described by Blake and Ollier (1971), tie channels connect the trunk of a river to floodplain lakes and are capable of bi-directional flow (Rowland, 2007). They have been shown to form from turbulent jet levee deposition, and have a unique single-channel, linear, narrow morphology (Rowland, 2007; Hull, 2016). Tie channels typically consist of clay-rich sediments, have v-shaped channels, and prograde basinward by continually eroding a cohesive prodelta (Rowland,

2007); these tie channels are documented at the Fly River in Papua New Guinea (Rowland & Dietrich, 2005), Birch Creek in Alaska (Rowland, 2007), and the Grijalva and Usumacinta River Basins in Mexico (Fig. 8) (Hull, 2016). Hull (2016) proposed that the single-thread, non-bifurcating nature of tie channels is due to the bedload of the channel lagging behind the mud in the system as a result of backwater effects. This restricts mouth bar formation in favor of levee deposition and subsequently promotes propagation of the single-thread tie channel.

Fig. 8. A tie channel prograding across a floodplain lake in the Grijalva River system, Tabasco State, Mexico (from Hull, 2016)

Elongate, single-thread lake deltas develop in man-made reservoirs throughout the United States (Fig. 9) (Tomanka, 2013). They look similar to tie channels, but build from the river into lakes as opposed to tie channels building off of rivers into floodplain water bodies. These single-thread lake deltas have an elongated morphology, signified by very low or zero bifurcation frequency and high length-to-width ratios. They are often supported by substantial levees on both

sides of one dominant channel. Therefore, they look like, and act like, a fluvial channel prograding into the basin as an extension of the river rather than a classical lobate delta deposit that fills all laterally available space. For this reason these systems will be referred to as fluvial-deltaic channels for the remainder of this paper. There are several models that propose explanations for the formation of elongate fluvial-deltaic channels or tie channels (Rowland et al., 2009; Falcini and Jerolmack, 2010; Tomanka, 2013; Canestrelli et al., 2014; Hull, 2016).

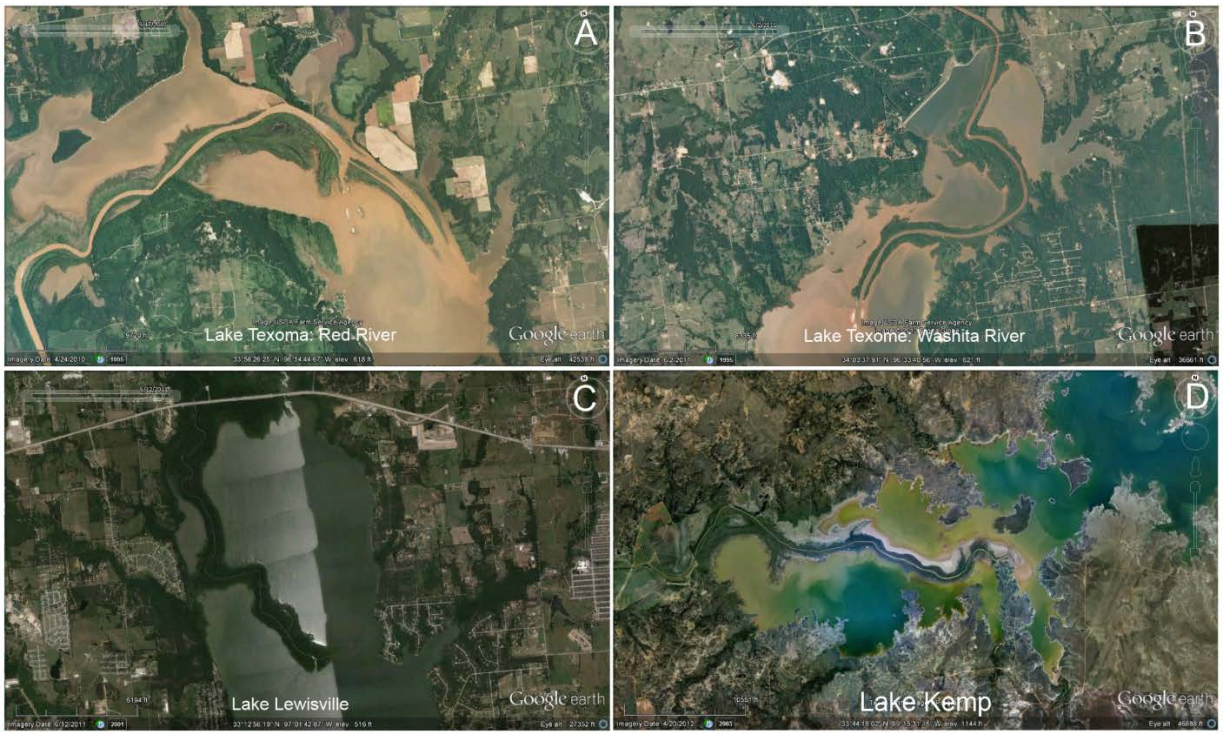

Fig. 9: Many elongate, single-channel deltas are forming in lakes throughout the United States (from Tomanka, 2013).

Rowland et al. (2009a) proposed three reasons tie channels are laterally stable and do not bifurcate, centered on the stability of the levees. First, tie channels initially incise into muddy prodelta deposits, “fixing” the channel location. Second, the levees are assumed to be made of stabilizing, cohesive, fine grained material. Third, vegetation further stabilizes the levees,

restricting lateral migration. These significant levee deposits focus the turbulent jet to continually erode river mouth deposits, promoting progradation without bifurcation.

Inspired by similarities of cold filaments of ocean currents that have structural integrity over long distances due to high potential vorticity, Falcini and Jerolmack (2010) developed a unique potential vorticity theory to explain jet sedimentation patterns of elongate channels. Their model merges the established hydrodynamic model of potential vorticity (Ertel, 1942) with sediment transport in order to predict sedimentation patterns. The equation incorporates channel width, channel depth, flow velocity, and suspended sediment concentration (SSC). Essentially, high potential vorticity flows retain the Gaussian velocity profile for longer distances, leading to less centerline velocity decay, and less mouth bar deposition due to higher shear stress in the center of the channel. High potential vorticity promotes advection within the flow; advection is the motion of particles along the bulk flow. Low potential vorticity promotes diffusive flow; diffusion being the net movement of particles from high concentration to low concentration. High potential vorticity flows with narrow channels, high SSC, and high flow velocity were found to produce focused levee deposition and subsequently elongate channels. Similarly, low potential vorticity with wide channels, low SSC, and low velocity are thought to be associated with frontal bar formation and bifurcation.

Canestrelli et al. (2014) linked river mouth depositional patterns to the stability or instability of the turbulent jet. They developed a stability parameter ‘S’, which is a function of friction (c_f, equation 1) and river mouth aspect ratio, inspired by the work of Jirka (1994). Their findings indicate that the stability of a river jet depends on both the stability parameter ‘S’ (equation 2) and the river mouth Reynolds number (equation 3). Using Delft3D simulation, stable jets with high stability parameters (high friction and high width/depth ratio) and low

Reynolds numbers formed mouth bars and bifurcating depositional patterns. On the other hand, unstable jets with low stability parameters (low friction and low width/depth ratio) and higher Reynolds numbers lead to higher transverse diffusivity, jet margin (levee) sedimentation, and elongate channels. Instable jets have advective effects, and stable jets have diffusive effects. They attribute elongated channels to the instable jets ability to build longer levees, focusing the jet, which moves mouth bar deposition further out from the mouth. The experiments reveal that jets delayed mouth bar deposition, but it is notable that they always formed eventually. This work determined a transition zone between stable and unstable jets by plotting deltas around the world by their respective calculated stability parameter and Reynolds number (Fig. 10).

(1) $\tau = \rho u^2 c_f/2$

(2) $S = c_f \frac{L}{h} = \frac{c_f}{2}\frac{B}{h}$

(3) $Re_B = \frac{U_0 B}{\nu}$

Notation

S	stability parameter
Re_B	Reynolds number
c_f	friction coefficient
h	channel flow depth (m)
B	river mouth width (m)
L	jet length scale (half river mouth width) (m)
τ	bottom shear stress (N/m^2)
ρ	flow density (kg/m^3)
u	jet centerline velocity (m/s)
U_0	cross section-averaged velocity (m/s)
v	molecular viscosity

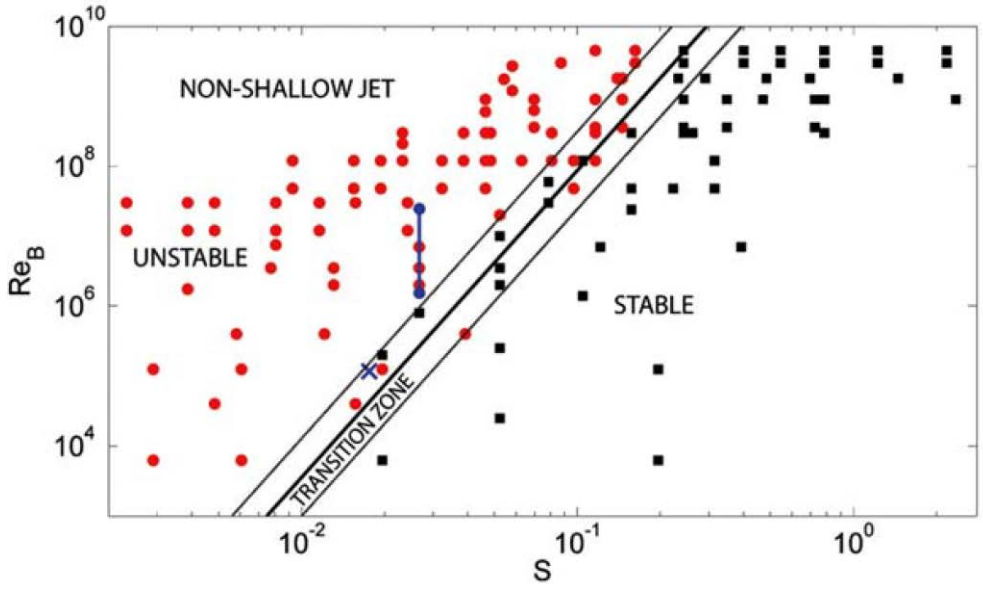

Fig. 10: Plot of deltas determined to have stable or unstable jet character plotted against their calculated stability number 'S' and river mouth width dependent Reynolds number. (from Canestrelli et al 2014).

Tomanka (2013) developed a model for the formation of single-channel prograding deltas based on his work on the Denton Creek Delta in Grapevine Lake. His model proposes that non-bifurcating deltas form by the turbulent jet eroding soft, semi-cohesive prodelta mud and simultaneously building sandy levees. During a large flow event, the orifice of the jet gradually moves upstream, widening the channel, which reinforces a basinward taper of the levees. These levees focus the jet, leading to sustained erosion of the mouth bar, deposition of sand on the channel flanks, and subsequently continued progradation without bifurcation (Tomanka, 2013). During a high flow event, elevated fluvial discharge would enhance the jet power to release upstream sediment and deposit thin, laterally continuous wing shaped sand sheets over the levees. He called these sand sheets blowout wings, and argued that they are a facies that should be associated with single-channel deltas forming in lakes.

Hull (2016) addressed the formation of tie channels in his study of wet, high-accommodation fluvial systems, specifically in his work on floodplain lakes of the Grijalva River system in Tabasco State, Mexico (Fig. 11). He argued that tie channels are propogating splay deltas that have a very low gradient which increases the upstream length of the backwater effect, diminishing the ability of the channel to transport coarse sediment. This results in sand (bedload) lagging behind clay (suspended load) in the channel. This sediment segregation causes mud to reach the river mouth first to form muddy, cohesive levees. These levees act to reinforce the elongation of the tie channel by focusing the jet to erode through the muddy prodelta deposits and continued starvation of the delta mouth for sand. During high-flow condition storm events, the muddy levees act as a "gun barrel" and are resistant to breaching; instead, the coarser sand bedload that was stored upstream will be deposited as overbank sheets, similar to the "blowout wings" described in Tomanka (2013).

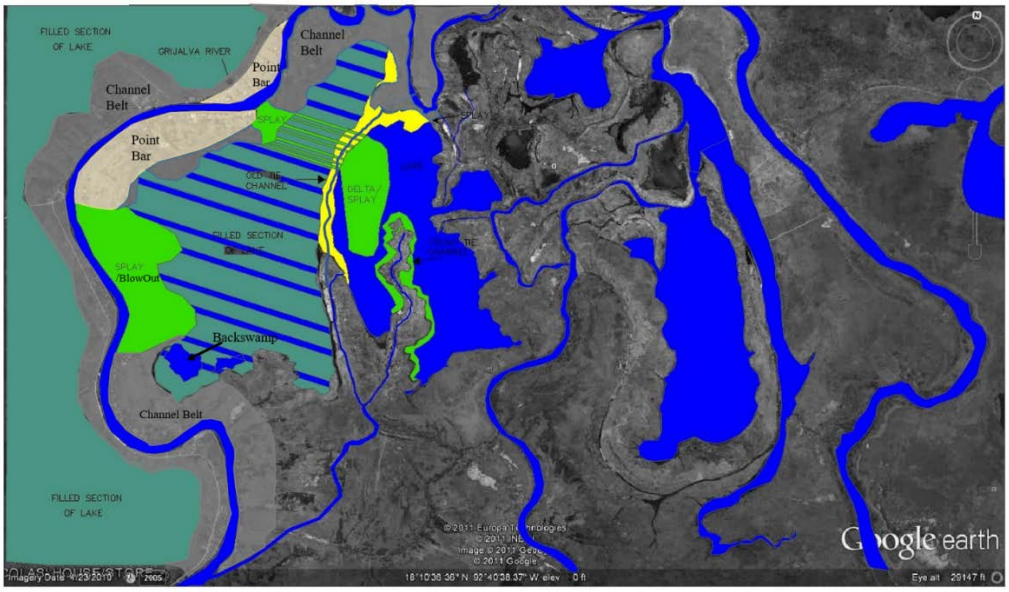

Fig 11. Floodplain lakes of the Grijalva River system, Tabasco State, Mexico. Tie channels were found to develop as prograding channels across the lake basin. Blowout wings, similar to those described in Tomanka (2013), were found to be associated with the evolution of these tie channels (From Hull, 2016).

The current state of research on elongate deltas shows a few commonalities. Elongated deltas are controlled by the processes occurring at the river mouth, specifically when subaqueous levees are formed in favor of frontal mouth bar deposition (Rowland et al., 2009; Falcini and Jerolmack, 2010; Tomanka, 2013; Canestrelli et al., 2014; Hull, 2016). Subaqueous levee deposition is proposed to be favored when the turbulent jet has high potential vorticity (Falcini and Jerolmack, 2010) or low stability (Canestrelli et al., 2014). Cohesion of finer grained sediment is a factor that enhances levee stability (Rowland et al., 2009a) and promotes delta elongation. Although there are field studies of tie channels (e.g. Rowland and Dietrich, 2005; Rowland, 2007; Day et al., 2008; Hull, 2016) and elongate deltas (Tomanka, 2013), there remains a notable lack of sedimentological data available from studies on elongated deltaic channels that can be used to correlate with and verify numerical models of their formation.

1.2. Study Areas

The field areas of Lake Texoma and Grapevine Lake were chosen for this study because they both currently have single-channel deltas prograding into their reservoirs.

1.2.1. Lake Texoma

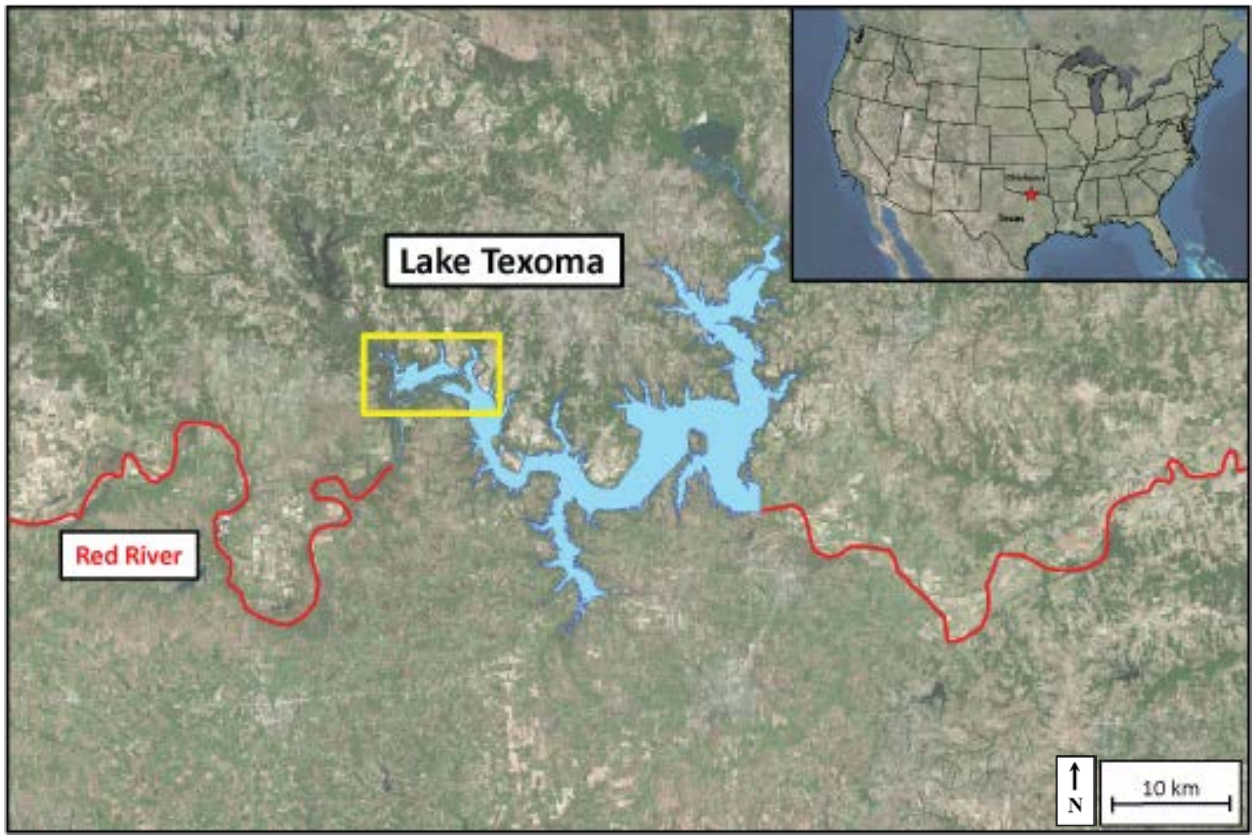

Fig. 12: Lake Texoma study area. The Red River Delta forms at the western edge of the basin, highlighted by the yellow box (Google Earth, 2017)

Lake Texoma is an artificial reservoir located along the state border between Texas and Oklahoma (Fig. 12). It is situated within Cooke and Grayson counties, Texas, and Bryan, Johnson, Love, and Marshall counties, Oklahoma. Beginning in 1944, the US Army Corps of Engineers dammed the water of the Red River to form Lake Texoma for the purpose of flood control, water supply, navigation, and hydroelectric power generation (USACE, 2016). The pre-

impoundment Red River and Washita River flowed unmodified through the area; the deepest portions of the modern lake represent the thalwegs of these rivers (Olariu et al., 2012).

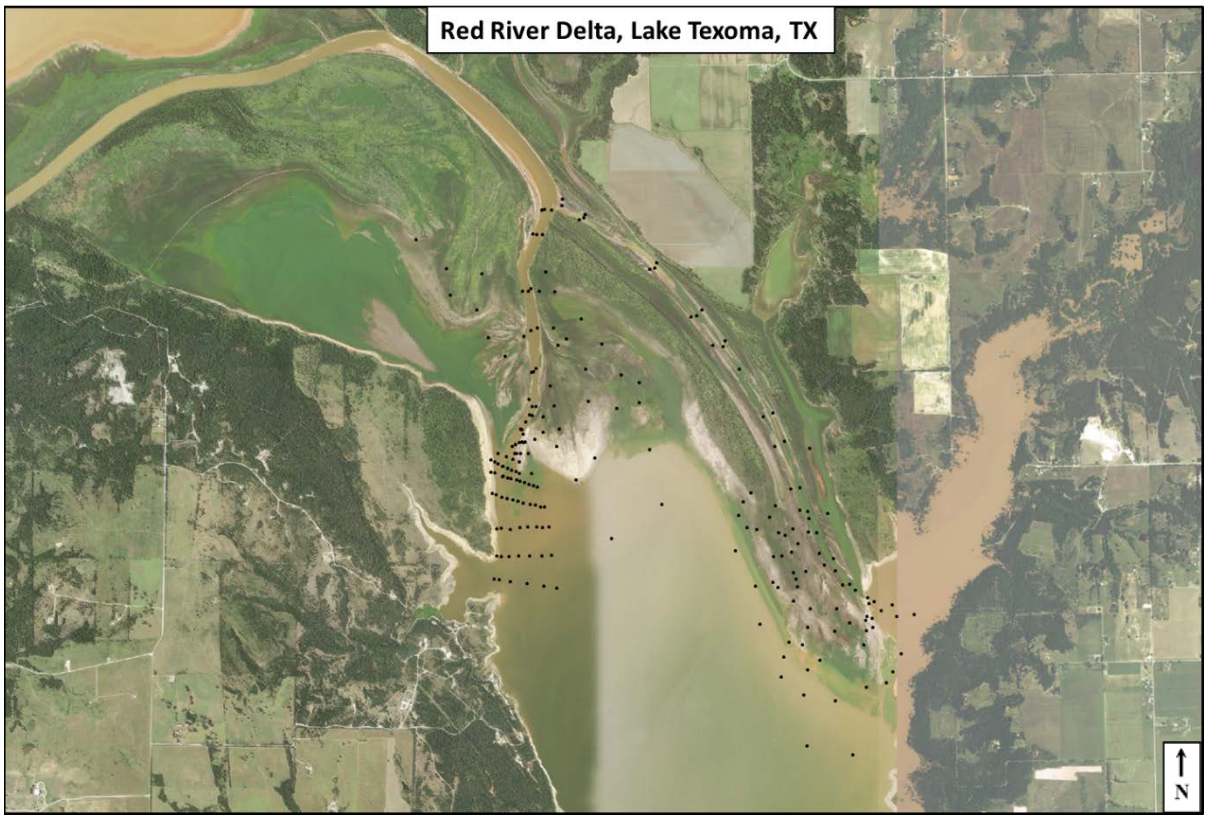

Fig. 13: The Red River forms an elongate, single channel delta into the lake basin. In 2004, the Red River avulsed. The abandoned delta channel runs along the eastern lake bank, and the active channel has cut through a splay delta and is currently prograding along the west bank (Image from Texas Natural Information Systems, 2014; processed in ArcGIS, 2017).

Conservation pool elevation for Lake Texoma is 188 ft above mean sea level (TWDB, 2002). The total storage capacity at conservation pool elevation for Lake Texoma in 1969 was 2,688,411 acre-feet with a surface area of 89,188 acres. The most recent Texas Water Development Board survey in 2002 determined that the current storage capacity has decreased 6.4% to 2,516,232 acre-feet with 16.3% lower surface area of 74,686 acres. This decrease in

reservoir storage is largely due to sedimentation from the Red River Delta in the northwest portion of the lake basin.

Lake Texoma has a total drainage area of 102,871 km^2 (TWDB, 1966), delivered to the basin primarily by the Red River with secondary contribution from the Washita River. The Red River is the dominant source of water to Lake Texoma, delivering an average discharge of 573 $m^3\ sec^{-1}$ into the reservoir (USGS National Water Information System; Fig. 3). The Red River flows over exposed Permian evaporates to the west of Lake Texoma, leading to an elevated total dissolved solids (TDS) and increased suspended-sediment concentration (SSC). This results in the influent waters of the Red River having a higher density than those of Lake Texoma. Therefore, the Red River delta is deposited as a constant hyperpycnal plume (Olariu et al., 2012).

Although Lake Texoma is an impounded basin, the Red River flows largely uninterrupted upstream of the lake. The Red River is 125 m wide before it enters Lake Texoma (Fig. 13). The Red River can be classified as a sandy, bedload-dominated river. It has a D_{50} median grain size of 2ϕ (0.25 mm), which corresponds to the boundary between fine and medium sand (Schwartz, 1978). This is illustrated by the presence of many mid-channel and side-attached bars located upstream of the river mouth (Fig. 14). The elongate geometry of the Red River Delta is a kind of paradox when the high sand load of the Red River is taken into account; sand-dominated rivers are traditionally expected to form lobate deltas owing to the tendency for sand to accumulate as mouth bar and drive bifurcation.

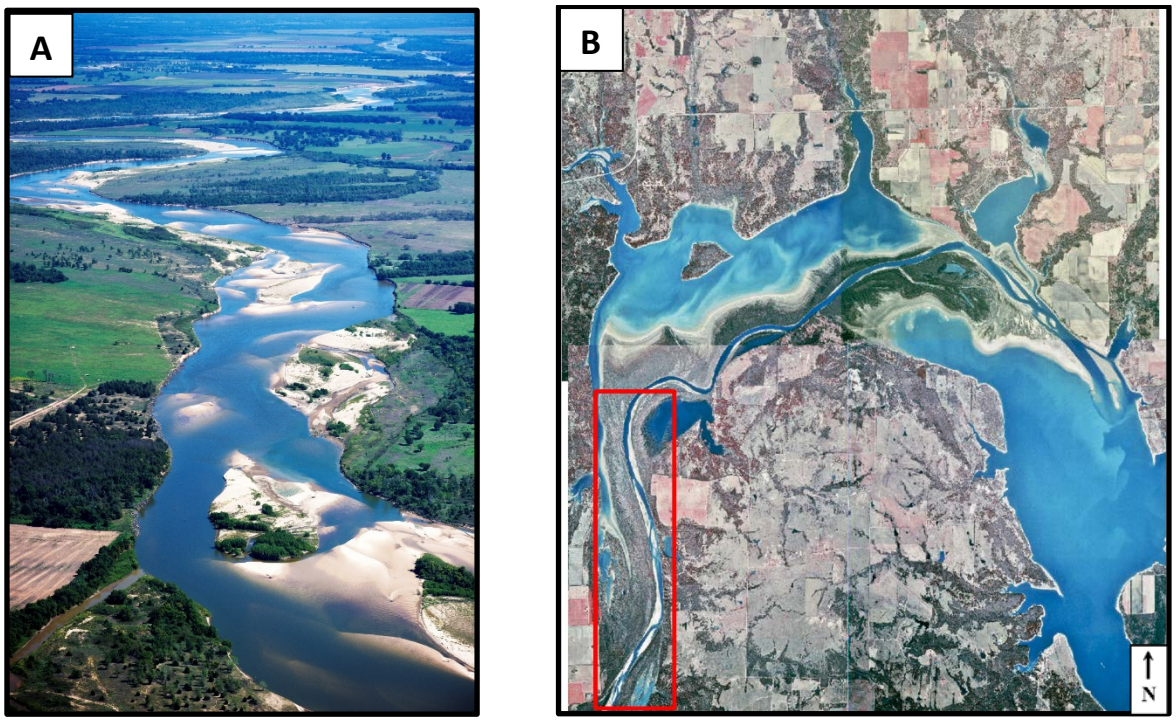

Fig. 14: (A) Image of the Red River taken upstream of Lake Texoma. The Red River is a sandy river with a high bedload (image by Henley Quadling). (B) Much of the sand in the Red River is stored upstream of Lake Texoma as mid-channel and side-attached bars (Image courtesy TNRIS, 1996; Processed in ESRI ArcGIS 10.4, 2017).

1.2.2. Grapevine Lake

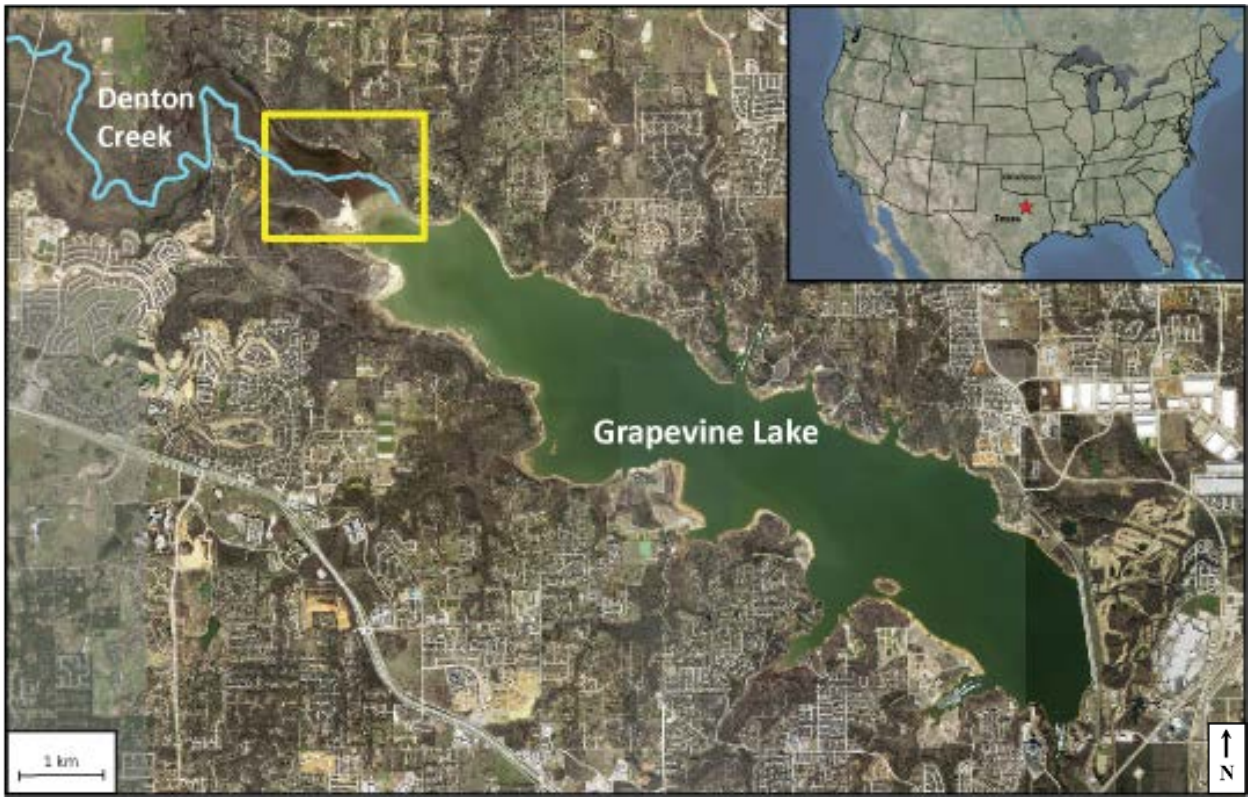

Fig. 15: Grapevine Lake study area located in Denton and Tarrant County, Texas, situated 20 miles northwest of Dallas, Texas (TNRIS, 2015).

Grapevine Lake is an artificial reservoir located in Denton and Tarrant County, Texas, situated 20 miles northwest of Dallas, Texas (Fig. 15). It was created by the US Army Corps of Engineers in 1952 by the impounding of Denton Creek, a tributary of the Trinity River, as part of a development project that included three other lakes in the area for the purpose of municipal water supply, recreation, and flood control of the Trinity River. Of the Trinity River's 720 mi^2 drainage basin located up dip of the lake, 695 mi^2 are accounted for by Grapevine Lake for flood control (USACE, 2017).

Fig. 16: The Denton Creek forms a prograding single-channel delta at the western edge Grapevine Lake (TNRIS, 2015).

Conservation pool elevation for Grapevine Lake is 535 ft above mean sea level (TWDB 2011). The total storage capacity at conservation pool elevation in 2011 was 163,064 acre-feet with a corresponding surface area of 6,707 acres. Since 1961, the total storage capacity has decreased 9.9%, corresponding to sedimentation by the Denton Creek Delta in the northwest portion of the basin (Fig. 16) (TWDB 2011).

Fig. 17: Aerial image of the Denton Creek Delta with channel sand locations overlain as orange polygons. Tomanka found that sand in Denton Creek was trapped upstream as bars and the river mouth was predominantly soft clay in comparison (Tomanka, 2013).

Denton Creek is a mud-dominated river with a higher proportion of the sediment moving through the system as suspended load relative to bedload. In general, the elongate morphology of the Denton Creek Delta is not dissimilar to that of the Red River Delta, but Denton Creek has a smaller median grain size. Tomanka (2013) noted that the sand in Denton Creek was choked upstream in the channel and only small amounts reach the river mouth (Fig. 17).

CHAPTER 2 – METHODOLOGY

2.1. Field Methods

2.1.1. Dutch auger coring

A Dutch auger coring system was used in order to identify subsurface lithology at the Red River and Denton Creek deltas. The Dutch auger is used to core up to 1 m of sediment below the surface. This is done by pushing the 2.5 cm diameter, semicircular gouge attachment at the end of the tool into the lake bottom, turning 360°, and pulling up using a separate T-shaped rod at the top of the tool. One meter extension rods permitted sampling at the 2-4 m lengths necessary for most samples (Fig. 18).

Fig. 18. Dutch auger cores were sampled for grain size at 10 cm increments, resulting in 10 sample points for each 1 meter core.

Sediment cores obtained with the auger were sampled at 10 cm increments. Grain-size analysis was performed at each 10 cm interval using the sense of touch technique (Thien, 1979). Grain-sizes are based on the USDA textural soil classification (Fig. 19). The color of each 10 cm increment was also logged using the Munsell color index (Fig. 20). Sedimentary structures and lithologic variations were recorded as continuous core.

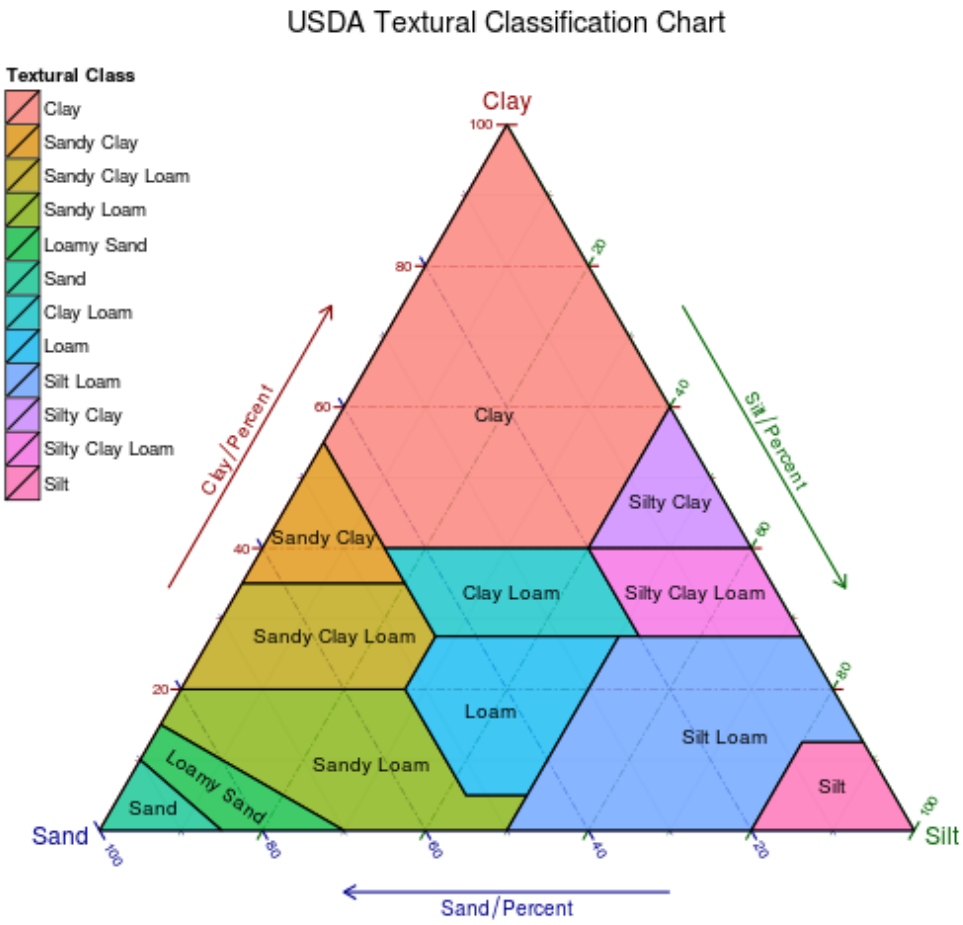

Fig. 19: The USDA Textural Triangle classifies sediments based on the relative abundance of sand, silt, and clay in the sample. This framework was used to classify cored samples of the Red River and Denton Creek Delta (Nicholas Hamilton, 2017)

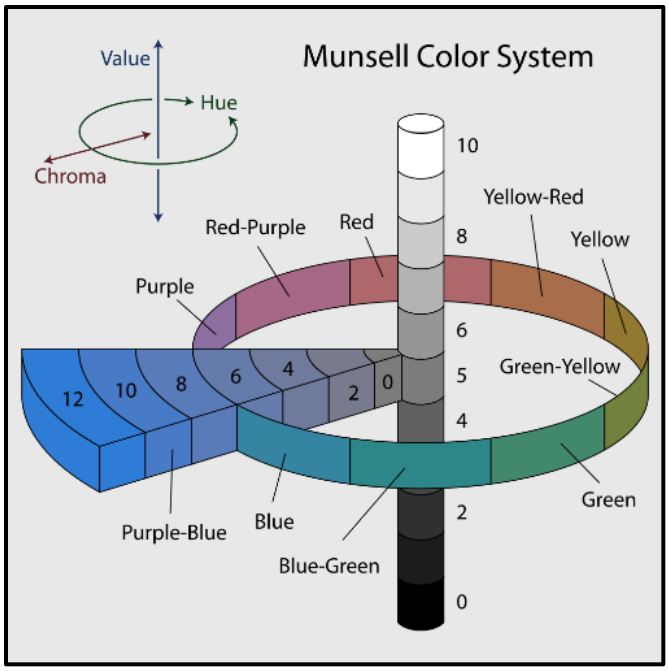

Fig. 20: The Munsell color system classifies colors based on hue, value (lightness), and chroma (color purity). It is used by the USDA as the standard color system for soils (Jacob Rus, 2017).

Due to the modern deltas at Lake Texoma and Grapevine Lake being perennially submerged in 15 to 25 ft of water, a boat was used to perform field measurements (Fig. 21). For this research, we used a 22 ft long Kenner fishing boat. Before sampling sediment, we deployed anchors on both the front and back of the boat to stabilize against the negative effects waves and wind.

A total of 277 Dutch auger cores were acquired. Of those, 246 were taken at Lake Texoma and 31 at Grapevine Lake. These samples were used to map lithologic variation across the Red River and Denton Creek deltas. Lithologic variations, particularly grain-size, is used to interpret changes in facies and, subsequently, depositional processes through time in these lacustrine deltas.

Fig. 21: A 22 ft fishing boat was used in order to access the actively forming portion of the Red River Delta and Denton Creek Delta for this study.

GPS data points were uploaded into ESRI ArcMap 10.4 software for visualization. The geographic coordinate system used was GCS North American 1983, and the projection used was NAD 1983 UTM Zone 14N. Sand isolith maps were created by displaying net sand percentages of individual core samples and contouring with colored shapes using the “create features” tool.

2.1.2. PVC Coring

More detailed and local analysis of sedimentary structures was facilitated with larger diameter cores collected with a separate coring tool (Fig. 22a). This suction core combined polyvinyl chloride (PVC) tubing, a PVC reducing coupler, and a metal check valve that attached to the T-handle from the Dutch auger system. The check valve was necessary to evacuate the

water column that builds above the sediment within the core when the core is taken subaqueously. Upon core extraction of the PVC tube with sediment, the check valve closes, and the tool can be retrieved without disturbance to the internal integrity of the core.

Four large cores were taken at the Red River Delta in Lake Texoma. Once the PVC core was in the lab, it was cut in half with a reciprocating saw. Half of the core is removed and a thin wire was used to clean the face of the sediment (Fig. 22b). This generated a 10 cm cross-sectional profile that revealed sedimentary structures as well as texture and color features. These cores were used to interpret relationships between depositional flow strength, grain-size trends, and bedding structures.

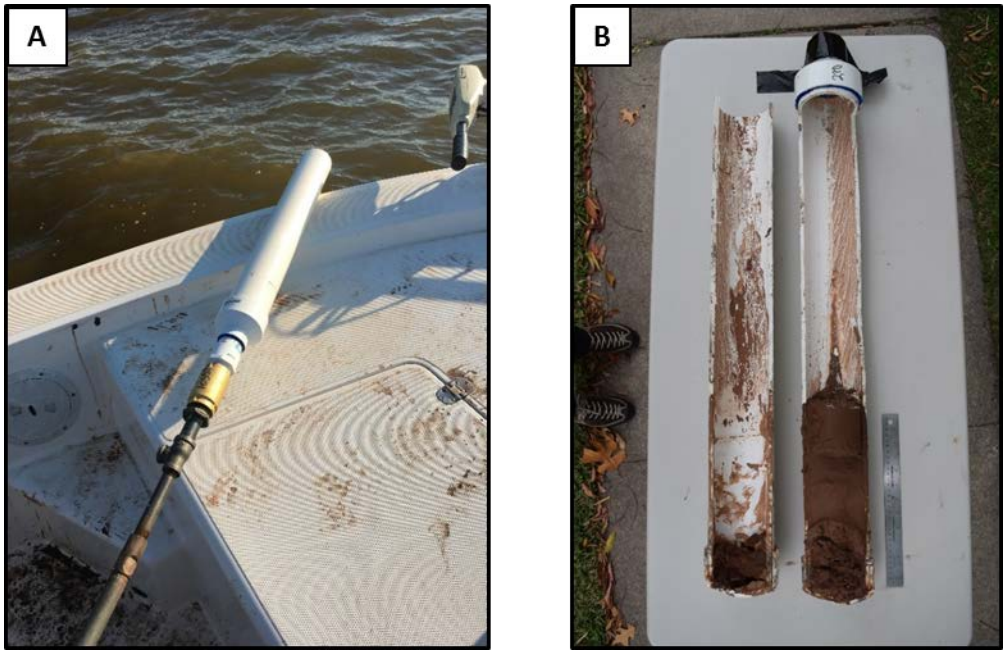

Fig. 22: (A) Coring apparatus consisting of a check valve connected to PVC tubing. (B) Following coring, the PVC tubes were cut in half with a reciprocating saw and cleaned with a thin wire for cross-sectional viewing.

Each sample location of Dutch auger core and PVC core were logged using a Trimble Geo7X H GPS, which has a 1 cm horizontal (x,y) and a 1.5 cm vertical (z) real-time accuracy.

2.2. Lab Methods

2.2.1 Historical imagery

Aerial photographic images were obtained and examined in order to observe the geomorphological history through time of the Red River Delta in Lake Texoma and the Denton Creek Delta at Grapevine Lake. These images were used to monitor channel avulsion and transitions between lobate and elongate delta morphology. Aerial images for the state of Texas are publicly available from the Texas Natural Resources Information System (TNRIS, 2017). The most recent images from 2015 are taken at 50 cm pixel resolution, with older images ranging from 1-2 m resolution. Aerial images for Lake Texoma were downloaded from TNRIS for Grayson and Cooke County, TX. This includes images for the years 1996, 1998, 2005, 2006, 2008, 2010, 2012, 2014, and 2015. Aerial images for Grapevine Lake were downloaded from TNRIS for Tarrant and Denton County, TX. Years covered are 1996, 2004, 2005, 2006, 2008, 2010, 2012, 2012, 2014, and 2016.

2.2.2. Hydrological data

Flow discharge data was obtained from USGS gauges in order to understand the relationship between river discharge and basin water levels of the two lakes in this study. The closest gauge upstream of the Red River Delta is USGS 07316000 near Gainesville, Texas. This gauge was used to collect Red River discharge data from 1990 to 2017. The velocity data is used to analyze the flow potential and fluctuation of the Red River through time. Basin water height was obtained from the USGS 07331600 gauge at Denison Dam near Denison, TX. This gauge

was used to identify changes in the height of the water level at Lake Texoma and by proxy the changes in elevation of the turbulent jet at the mouth of the Red River Delta.

CHAPTER 3 – RESULTS

3.1. Lake Texoma

3.1.1. Historical imagery and delta events

Aerial photographs show a prograding Red River channel formed along the northeast bank of Lake Texoma in 1984. In 1995, the levee of the prograding channel was breached, the existing channel to the east was abandoned, and a lobate delta began to form to the southwest (Fig. 23). The lobate delta formed from sediment derived from the breached levee. This was followed by the formation of a step down, falling stage lobate delta that laps onto the face of the first delta. After the distributive phase of the two lobes ended in 2011, channels of the two splay deltas coalesced into a new prograding channel that cut through both lobes and persists today along the southwest bank of Lake Texoma.

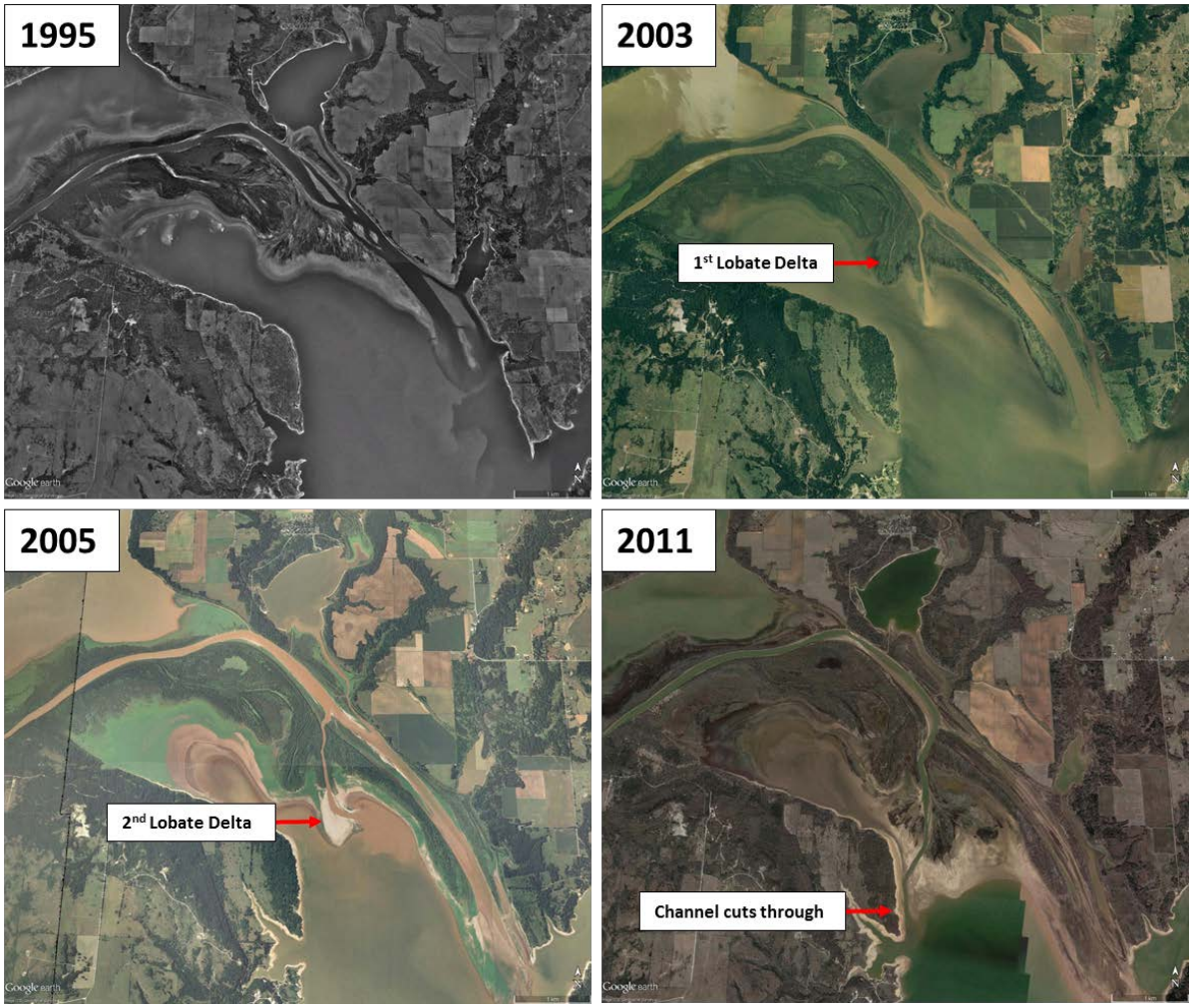

Fig. 23: Time series of the Red River Delta. In 1995 the Red River Delta avulsed and began to form a lobate delta. Between 1995 and 2003 a second, falling stage delta formed. In 2011 the delta channel cut through the lobate deltas and returned to a prograding channel morphology.

3.1.2. Red River Delta Stratigraphy

Sediment textural mapping reveal four trends in the sediment distribution of the Red River Delta (Fig. 24). Sand is absent at the delta front of both the abandoned eastern delta channel, as well as the active western delta channel. Sand deposits accumulate upstream of the river mouth within the channel as mid-channel and side-attached bars. Laterally distributed sand

is present near the location of the 1995 avulsion in the two contiguous splay deltas. The overwhelming majority of the sand in the Red River Delta proper occurs as thin sheets atop and beyond the levees in the basin and lateral to the main channel.

There is a distinct absence of sand in the river mouth of both the abandoned western channel and the active eastern channel of the Red River Delta. There are small amounts of sand (1-15 cm) in the mouth of the active western channel, but they are thin stringers within a matrix of mud and constitute less than 10% of the upper meter of sediment at and basinward of the delta channel mouth. Cores taken in and lakeward of the mouth of the abandoned eastern channel produced homogeneous mud plugs with no discernable sand layers.

The amount of sand in the channels decreases gradually from the avulsion location towards the mouth of both delta channels. Near the location of the 2004 avulsion (# symbol, fig. 24), there are two large mid-channel sand bars (+ symbols, Fig. 24) lining the bottom of both the west and the eastern arm of the Red River Delta channel. These bars are elongated with the long axis in the flow direction. Cores in these bars are generally sand rich with up to 75% sand in the middle of the bars. Within the active eastern delta channel, there are small sand bars positioned where the channel progradation deflects slightly from linear (& symbols, Fig. 24). This slight meandering of the eastern delta channel reflects side-attached bars on both the inside and outside bends. The sand bars in the delta channel decrease in size from the avulsion node towards the river mouth.

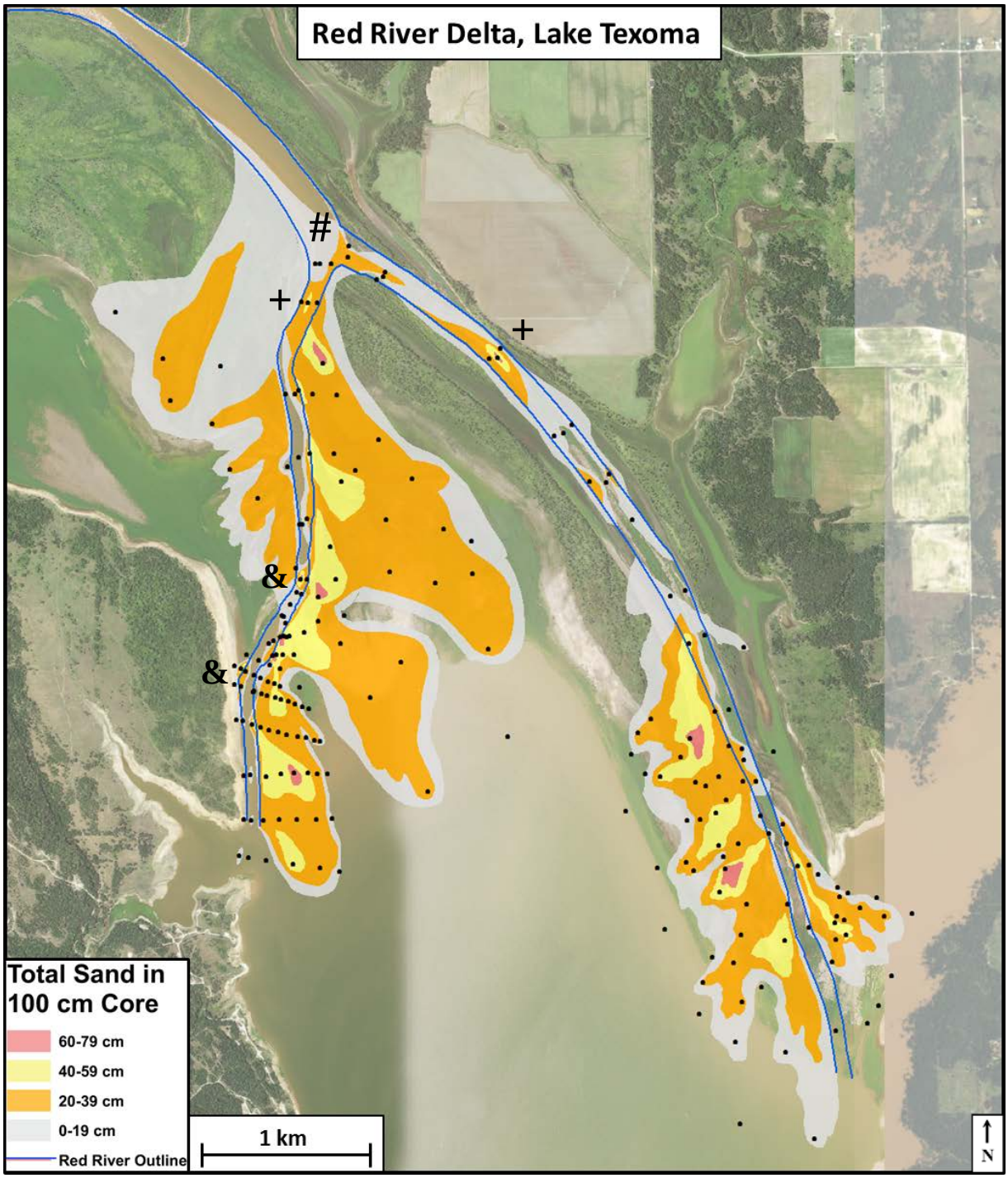

Fig 24: Sand isolith map of the Red River delta. The channel to the east was first deposited, followed by an avulsion that initiated the western lobe as a splay delta. The splay delta then evolved into the linear delta that persists today. Notable depositional trends are a lack of sand at the river mouths of both deltas and sand sheets on top of and extending beyond the levees.

Near the 1995 avulsion (Fig. 23), there are two stacked splay deltas. These two parasequences are composed of three coarsening upwards lobes built on each other (Fig. 26). In a longitudinal cross section (Fig. 26), these sand lobes have a vertical stacking, fining upwards sequence of sand overlain by silts, loams, and clay. The geometry of these deposits in a strike cross section (Fig. 25) is lens shaped and lobate, with the thickest sands near the channel that thin away. There are occasional roots and mud clasts within the loam and clay layers. Since the delta channel has cut through the splays, lake mud has lapped onto the top of the final sands of the second splay. These deposits correspond to the 1995-2011 lobate delta period of the depositional sequence.

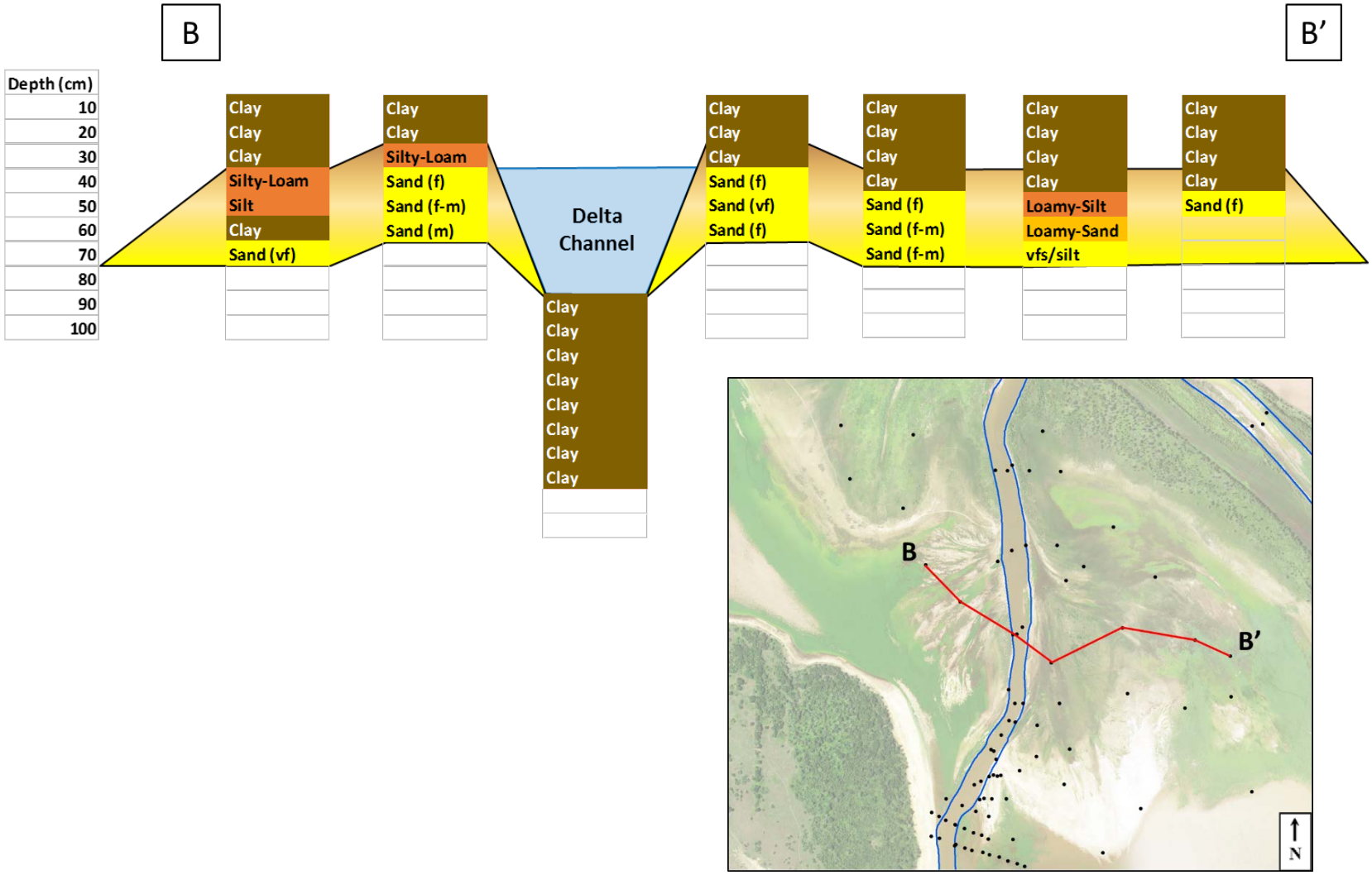

Fig. 25: Strike cross section from B to B' across the splay delta that penetrates to the top of the upper most sand and shows muddy lake deposition on top of the last splay that has occurred since the delta channel cut through the splays.

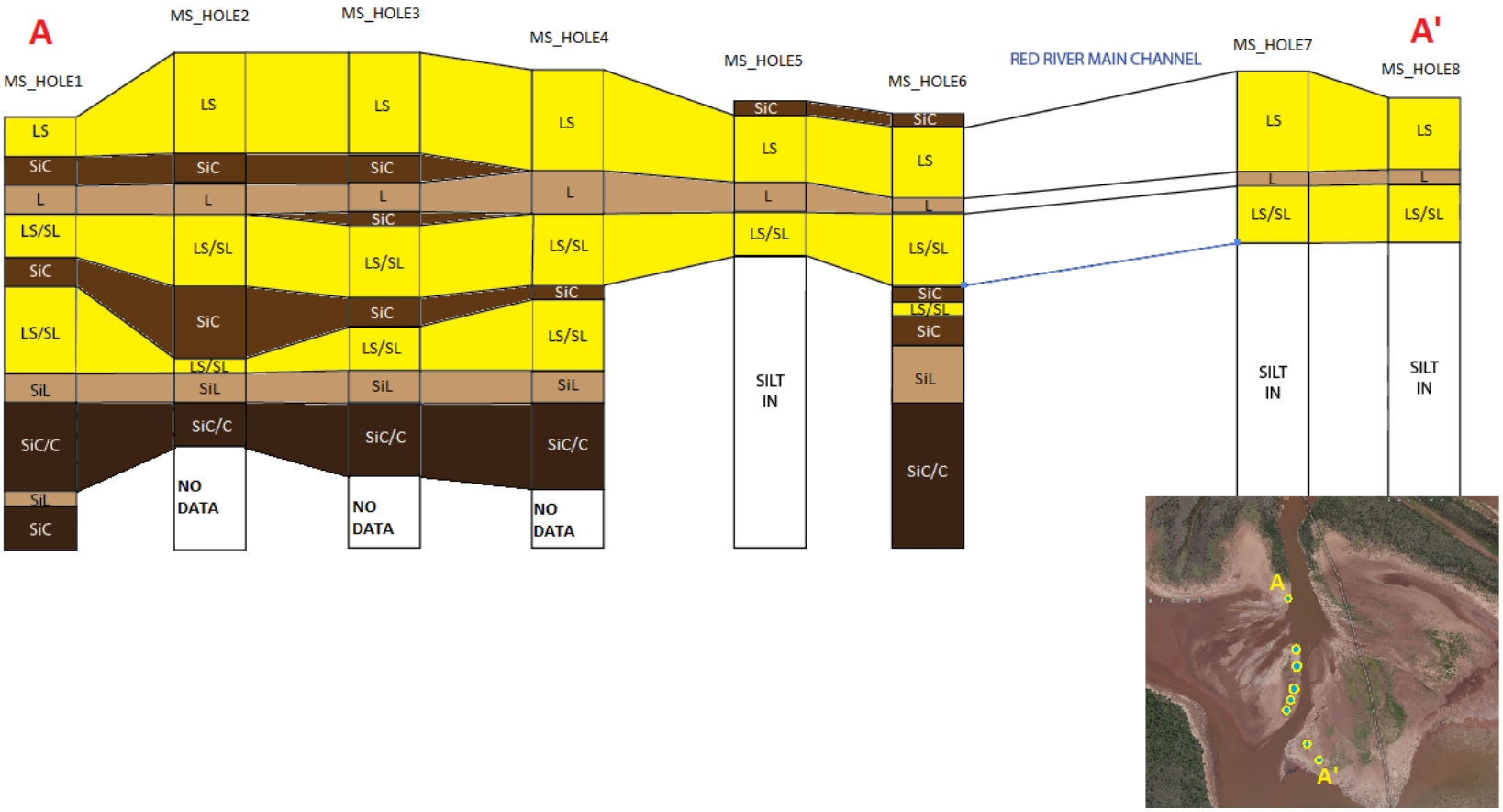

Fig. 26: Longitudinal cross section of the splay delta. Splay delta lobes show vertical stacking of coarsening upwards packages.

Sand was found in abundance lateral to the delta channel as thin sand sheets. These sands sheets are thin (10-40 cm) and laterally continuous, extending from the channel over the levees up to 700 m into the basin (Fig. 27). We acquired three of the larger suction cores along these wings from locations ranging from proximal to more distal from the delta channel (Fig. 28). The first core was retrieved most proximal to the channel and is made up of a clay base overlain by 40 cm of fine to medium sand that grades from silt to clay at the top (Core 1, Fig 28). The sand deposit has a sharp basal contact, followed by climbing cross ripples throughout most of the deposit. A teepee structure recording fluid escape is found near the top of the sand interval. Core 2 was retrieved at an intermediate distance from the channel. It is made up of a clay base with 18 cm of fine to medium sand that is topped by clay (Core 2, Fig 28).. The basal contact between the clay and the sand is sharp. The sand has semi-convolute laminations with rip up clasts of mud and organic matter embedded within. The sand interval is homogeneous in terms of grain size variation. The top contact between the sand and the clay is sharp. Core 3 was retrieved at an intermediate-to-distal distance from the delta channel. It is made up of a clay base, 20 cm of fine sand and silt, and capped by clay (Core 3, Fig 28). The basal contact between the clay and the fine sand is sharp. There are notable amounts of ripple lamination, rip up clasts, and organic matter throughout the sand and silt section. The top of the fine sand and silt interval grades into clay.

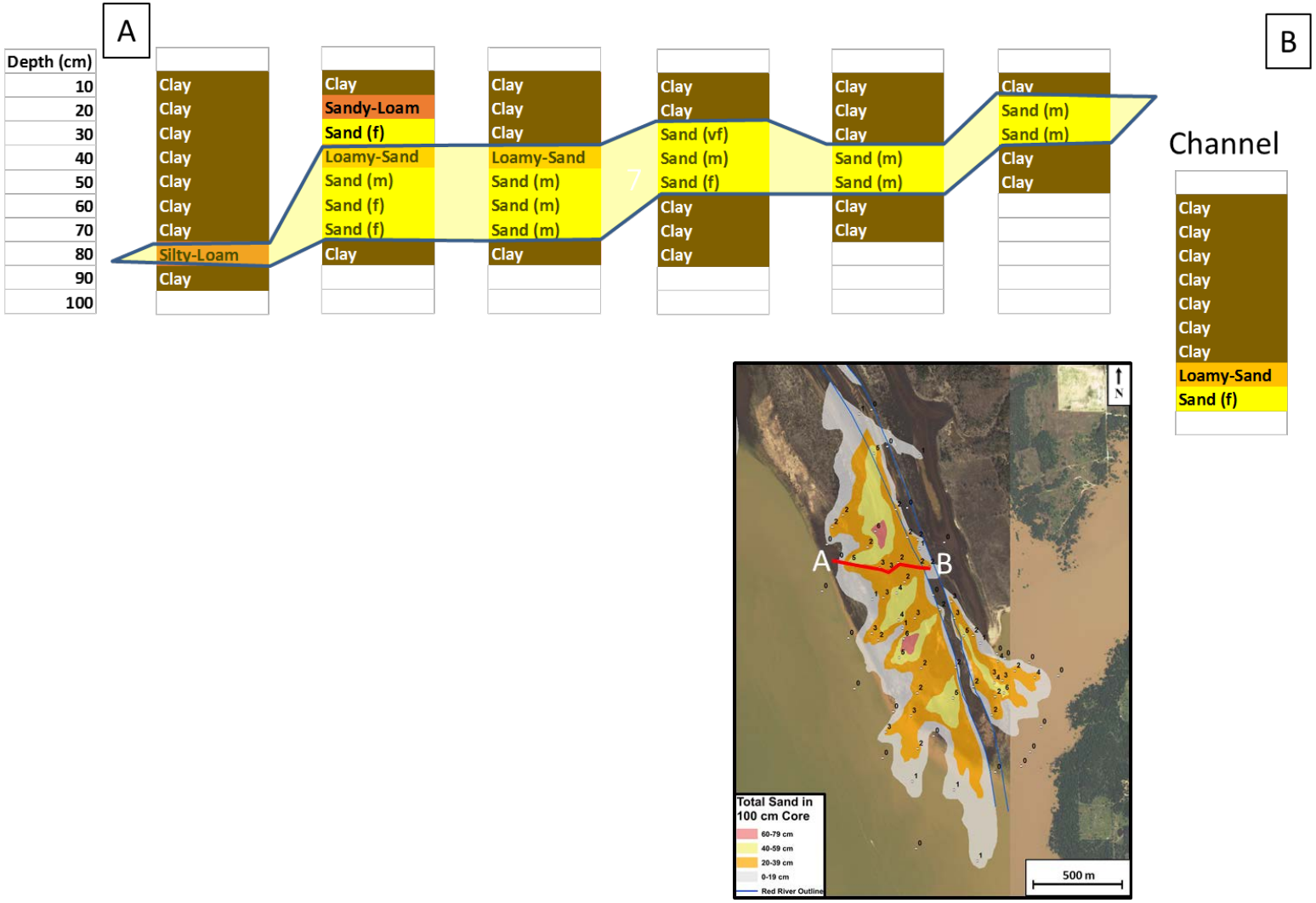

Fig. 27: Cross section across a representative blowout wing. This wing is 20 to 40 cm thick, encased in lacustrine clay, and has a width of ~500 m perpendicular to the channel axis.

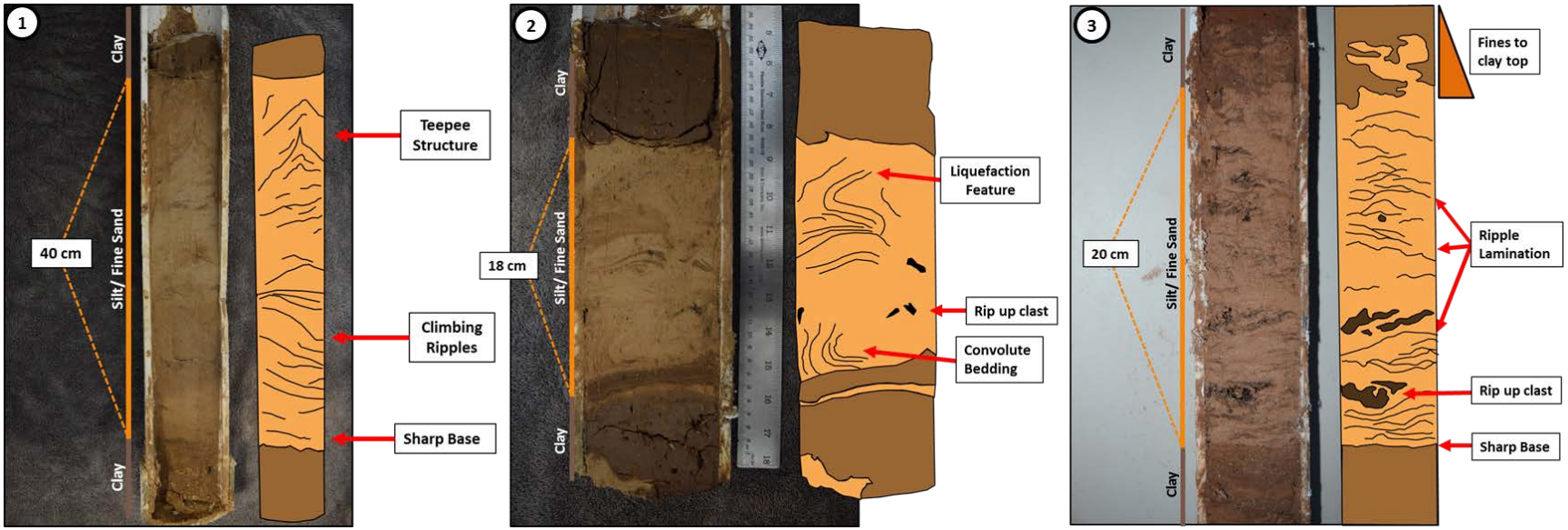

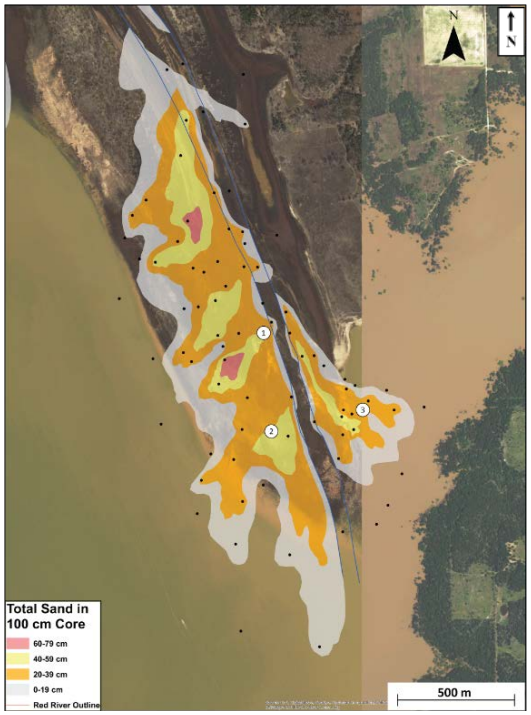

Fig. 28: Core 1: Proximal blowout wing. Proximal to the distributary channel, the blowout wing is made up of fine to medium clean sand, has a thickness of 40 cm, shows a sharp basal contact with underlying lacustrine clay, and progresses through claiming ripples into a teepee structure at the top. The top contact is gradational from silt to clay.

Core 2 – Intermediate blowout wing. Further from the channel, the blowout wing has tapered to 18 cm of fine to medium sand. The basal contact is sharp with the underlying lacustrine clay. The wing has convolute bedding, rip up clasts of consolidated mud and organics, and has a sharp upper contact with more lacustrine clay. Near the top of the sand wing is a liquefaction feature with increasingly high angle laminations.

Core 3 – Intermediate-distal blowout wing. Furthest from the channel, the blowout wing has a thickness of 20 cm of fine to medium sand. The basal contact is sharp with the underlying lacustrine clay. The wing has strong ripple lamination throughout, rip up clasts of consolidated mud and organics, and gradationally fines to clay at the upper contact.

3.2. Grapevine Lake Results

3.2.1. Denton Creek Delta Sand Sheets

Investigation at Grapevine Lake was focused on mapping of sand sheets previously identified by Tomanka (2013) as blowout wings (Fig. 29 & 30). These sand sheets were the first recognized blowout wings and, though he did not have the opportunity to map their distribution, their identification by Tomanka (2013) prompted the investigation for similar wings at Lake Texoma.

In this work, our mapping of the Grapevine Lake blowout wings show that they extend 200 m perpendicular from the channel and 375 m along the channel axis (Fig. 31). Each auger core sample taken within a wing was composed of moderately to highly homogeneous sand, reaching ~80 cm sand content out of 100 cm cores. The thickest sand deposits were nearest the channel, and the proportion and thickness of sand diminished away from the channel (Fig. 32). In cross section, we map one discrete wing with thickness ranging 20-40 cm, composed dominantly of sand and lesser sandy loams encased in mud. The long axis of these wings is perpendicular to the channel, similar to the wings at Lake Texoma. There was a lack of sand found in the current Denton Creek channel. The absence of sand in the delta channel is consistent with the findings of Tomanka (2013), who documented a gradual decrease of sand in the downstream direction within Denton Creek.

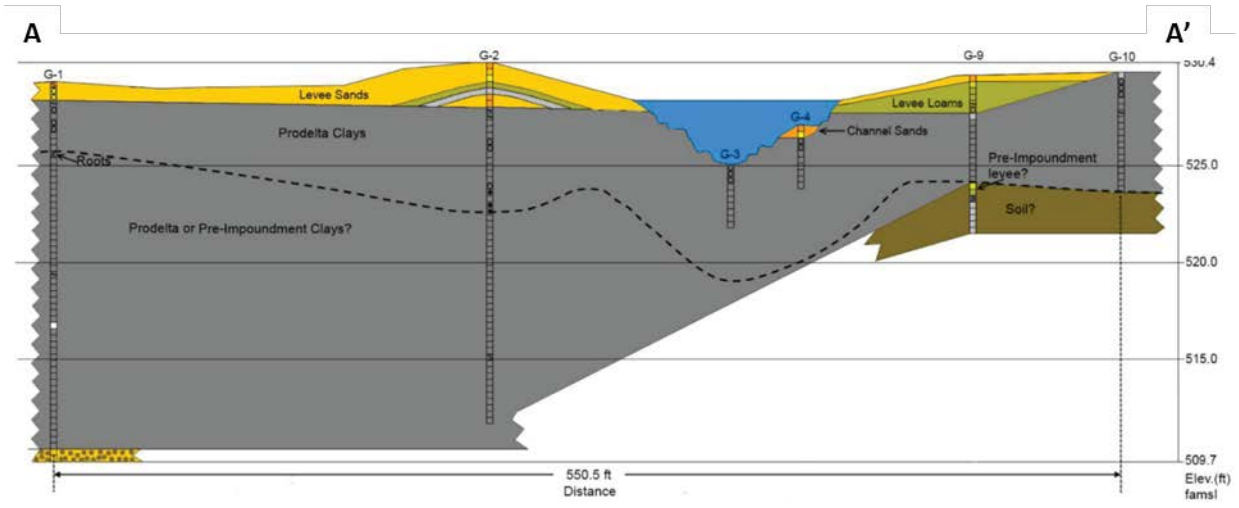

Fig. 29: Cross section from A-A' marked on the sand isolith map. Sand sheets are found atop and beyond the levees reaching into the basin (Cross section from Tomanka, 2013).

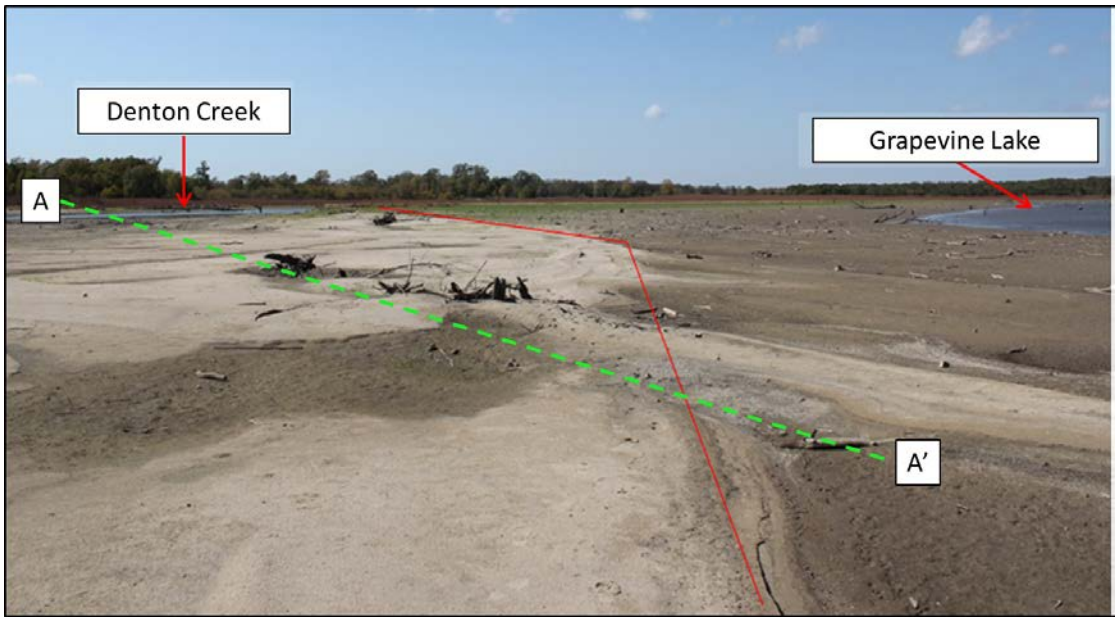

Fig. 30: Image of a blowout wing taken following a storm event at Grapevine Lake (from Tomanka, 2013). General location of Fig. 30 A-A' cross section marked as green dashed line.

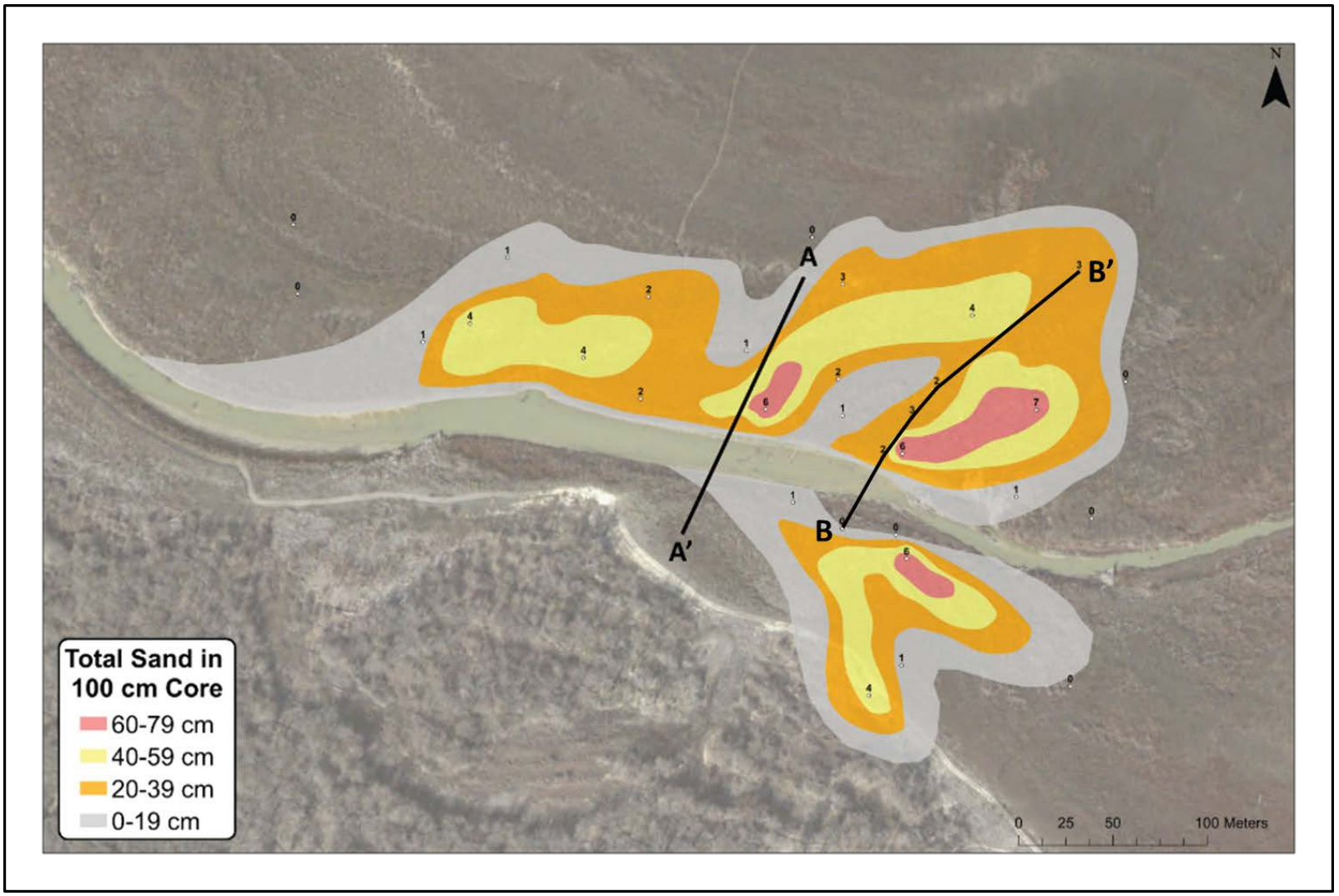

Fig. 31: Sand isolith map of Grapevine Lake blowout wings. Cross sections for figures 28 and 31 marked on map.

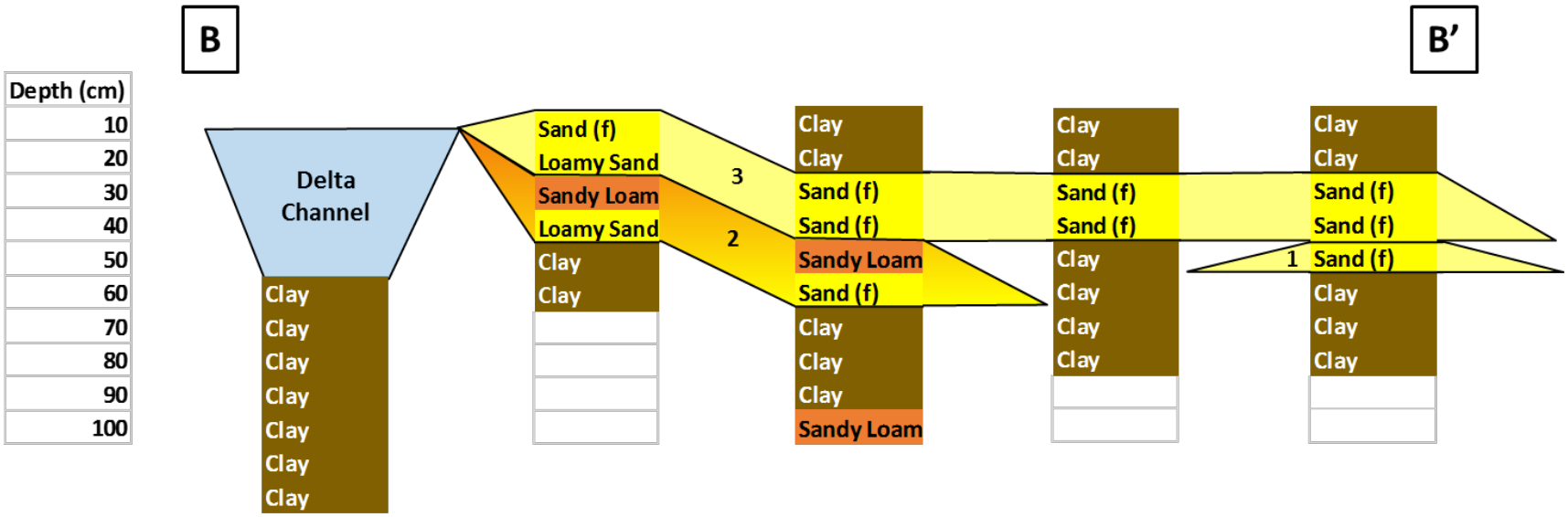

Fig. 32: Cross section B'B' of two stacked wings that are from the same breach. Wing 1 is from the upstream wing. Wing 3 laps onto wing 1.

CHAPTER 4 – DISCUSSION

Part one of this discussion details the four architectural elements of the Red River Delta at Lake Texoma and Grapevine Lake and proposes a depositional origin for each. Part two of this discussion places these elements in the context of a depositional model.

4.1. Architectural elements of a single-channel fluvio-lacustrine delta

Based on the field observations at Lake Texoma and Grapevine Lake, we interpret four distinct architectural elements that comprise the single-channel delta system and may be representative of elongate lacustrine deltas as a whole (Fig. 33). (1) prodelta/ lake muds, (2) splay delta, (3) fluvio-deltaic channel fill, and (4) overbank sand sheet – "blowout wings".

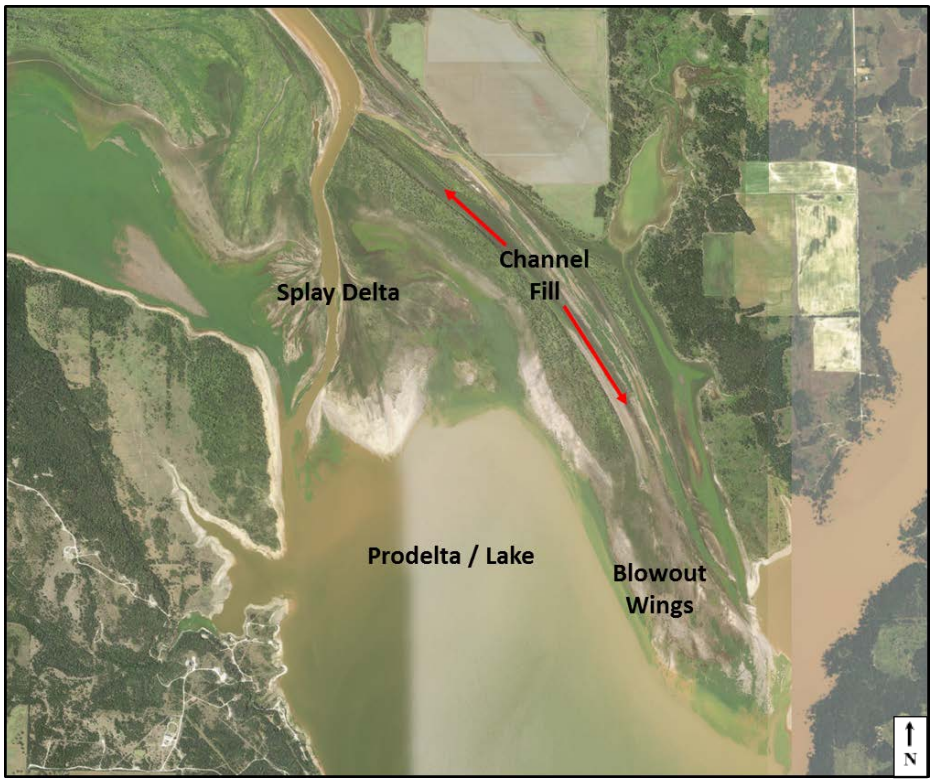

Fig. 33: The Red River Delta is composed of 4 architectural elements: prodelta / lake, splay delta, distributary channel fill, and overbank sand sheet or "blowout wings".

4.1.1. Architectural Element 1: Prodelta / Lake

Prodelta / Lake Mud Description

Open lake deposits comprise a significant portion of the Red River Delta. Every core sampled beyond the current extent of the prograding delta channel was 100 percent mud. These muds show a lack of both rooting and soils. Cores taken near the mouth of both the abandoned and active channel of the Red River Delta produced consistent mud plugs of 90-100 cm out of a 100 cm core. Most of the clay was highly liquid and had yet to harden, resulting in a generally soupy texture. Tomanka (2013) also reported semi-cohesive, unconsolidated mud and loams within the river mouth and prodelta of Denton Creek at Grapevine Lake. These open lake deposits are highly fluid and easily eroded. Auger coring was limited to 1 meter of the subsurface, but these water-saturated muds may extend deeper, but no deeper than the pre-impoundment surface, overlying the previous river floodplain deposits. These lake mud deposits will conform to the shape of the basin they are filling. All sands deposits are encased in this lacustrine mud.

Prodelta / Lake Mud Interpretation

These open lake muds are a result of subaqueous deposition, indicated by the lack of rooting and soils. The vast majority of the bedload sand in the Red River is found upstream of the river mouth, and deposits beyond the river mouth in the open lake are devoid of sand sized sediment. These muds are deposited when suspended clay particles reach the river mouth to be incorporated into the turbulent jet and settle from the decelerating jet waters. These muds outpaced bedload sand in this delta system and accumulate before sand progradation. No sand reaches the delta mouth, so no mouth bar sands are accumulated and sand only progrades over

mud upon override of the channel. This lake mud represents deposition in front of the delta before channel progradation but also includes levee overbank mud deposits later.

4.1.2. Architectural Element 2: Splay Delta

Splay Delta Description

Two splay delta elements are found near the avulsion node at the Red River Delta. The splay complex has a planform width of 1,100 m and length of 1,200 m. These delta deposits have a lobate, lensoid geometry horizontal to channel flow and a vertical stacking of one or more coarsening upwards sections of loamy sands over silty clay and loams (Fig. 26). The deposit is lobate, with the width of the splays increasing downstream from the location of avulsion. The thickest sands are nearest the channel. Roots and mud clasts are interspersed within. The splay deposit is capped by lacustrine mud.

Splay Delta Interpretation

These splay deltas record a distributive delta phase following the 1995 avulsion. These lobate deltas form out of the readily available sandy sediment in the channel at the breached levee. The high local concentration of sand to redistribute forced the system to form significant mouth bars and bifurcate into multiple distributary channels. The sediment from the breached levee was fully distributed as a splay delta into the adjacent lake. The channel extended through the first delta and deposited a second splay delta in front of the first but at a lower lake level. The avulsed Red River delta channel cut through these two splay deltas and returned to a single-channel progradational morphology.

4.1.3. Architectural Element 3: Fluvio-deltaic channel fill

Channel Fill Description

Sediment within the delta channels form mid-channel and side-attached sand bars. These sand bars have a thick center and thin to the edge, forming a lens geometry with the long axis in the direction of flow. The sand bars have a high percentage of clean sand. Where there are not sand bars within the channel, cores are dominated by clay and minor silts. At Lake Texoma, there is a gradual decrease of sand from the avulsion node to the river mouth; sand bars become smaller and less frequent in the downstream direction. The abandoned eastern delta channel is currently filling with mud and organic matter on top of the sand bars present before avulsion. Less than a meter of sediment has accumulated in the abandoned Red River channel so far. At Grapevine Lake, there was also a documented loss of sand in the downstream direction towards the Denton Creek river mouth (Tomanka, 2013). The sand deposits in Denton Creek are less frequent and progressively smaller in size and thickness as nearest the river mouth.

Channel Fill Interpretation

Although fluvio-deltaic channels in the Red River delta do not to bifurcate, they do avulse. When this happens, the original distributary channel is abandoned and a new active channel is formed. The abandoned channel will be prone to still water deposition owing to the loss of active flow. The channel deposit will consist of the sand bars left in the channel where they were during the time of avulsion, no longer migrating downstream due to the loss in flow. These bars will be buried by the clay-rich portions of the channel following the avulsion. Clay-rich fill is a heterolithic deposit consisting of clay, loam, silts, and minor amounts of sand that

accumulates on top of the original sand bars and clay. These channel fills scour into the prodelta lake mud elements.

4.1.4. Architectural Element 4: Overbank Sand Sheets / Blowout Wings

Overbank Sand Sheet Description

Overbank sand sheets extend laterally from the delta channel axis. These sand sheets are 10-40 cm thick (Fig. 28) and are composed of clean fine-to-medium grained sand that often fines into sandy loam and silt. Core samples of the wings show a sharp base of sand on top of clay. The dominant sedimentary structure within the wings are ripples, with lesser amounts of rip up mud clasts and organic debris. Fluid escape structures are increasingly common at the top of the cores, indicted by near vertical laminations. The wings are capped by a transition from the fine sand into silts and clay. They have depocenters near the channel just off the levees where the sand in discrete sheets is thickest and thins gradually away from this center. Likewise, discrete sheets constitute sand bound by muddy strata (Fig. 32).

Tomanka (2013) identified these overbank sand sheets at Grapevine Lake with the shape of wings deposited with widths up to 600 ft (183 m) perpendicular to the channel. Analogous overbank sand sheets are found perpendicular to tie channels within the Grijalva River system in Tabasco State, Mexico (Hull, 2016). Hull (2016) named these extensive sand sheets “blowout wings” and suggested they play an integral role in the sustained progradation without bifurcation of tie channels. We propose the overbank sand sheets at the Red River Delta are analogous blowout wings to those first described by Tomanka (2013) and expanded on by Hull (2016).

The blowout wing complex at Lake Texoma comprises 5 distinct sheets representing at least 4 separate depositional episodes. The last two wings could be deposited during the same depositional episode, one on each side of the channel. The aerial dimensions of the blowout wings at Lake Texoma are measured by two parameters. First, the length is defined as the size of the sand sheet parallel to the channel axis or flow direction. Second, the width of the wing is measured as the size of the wing in the perpendicular direction from the channel axis. Using these definitions, the 5 sheets have an average length of 778 m and an average width of 556 m (Fig. 34). Using the Red River channel width (W_C) of 125 m we normalize these dimensions to a length of 6.2*W_C and a width of 4.4*W_C. These measurements correspond to a 1.4 length/width ratio. Using the average thickness of 26 cm (0.26 m) for the 4 blowout wing cores, the aspect ratio for these wings is 2,480 (2,480 m wide per 1 m thickness).

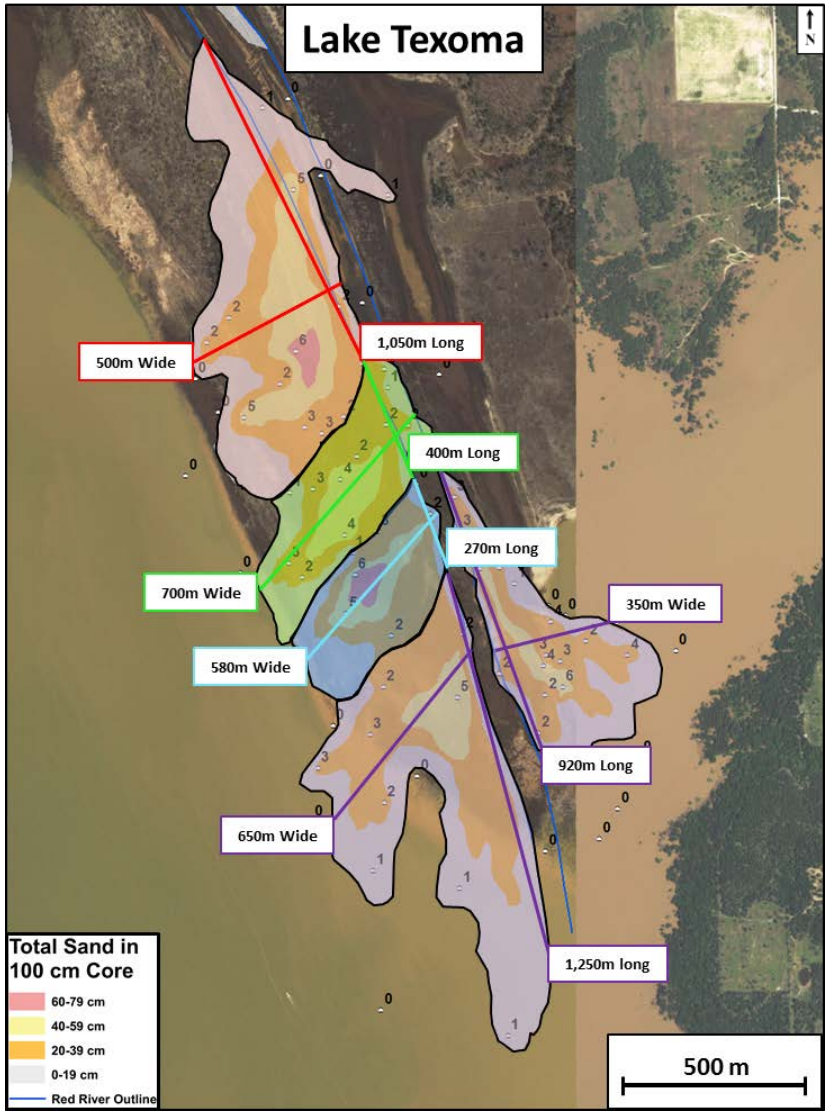

Blowout Wing Dimensions	
Length (m)	Width (m)
1,050	500
400	700
270	580
1,250	650
920	350

778m avg length (6.2x channel width)
556m avg width (4.4x channel width)
1.4 length/width ratio

Aspect Ratio
2,480m wide: 1m thick

Fig. 34: Lake Texoma blowout wing dimensions have an average length of 778 m and width of 556 m. They have an average length-to-width ratio of 1.4, and aspect ratios of 2,480 (2,480 m per 1 m thickness).

The blowout wings at Grapevine Lake displayed a similar pattern to those at Lake Texoma with the thickest sand at depocenters and thinning away from this focal point. Mapping reveals 3 overbank sand sheets at Grapevine Lake corresponding to 3 separate depositional episodes (Fig. 35). These 3 wings have an average length of 125 m and an average width of 127 m. Using the Denton Creek channel width (W_C) of 25 m, these dimensions scale to a length of $5*W_C$ and a width of $5.1*W_C$. Using the average thickness of 26 cm (0.26 m) for the 4 blowout wing cores, the aspect ratio for these wings is 633 (633 m wide per 1 m thickness)

Although the sand sheets at the Red River Delta, Lake Texoma and the Denton Creek Delta, Grapevine Lake vary greatly in size, they have striking similarities. The Red River is 5 times as wide with a 125 m channel width upstream of the Red River Delta, and Denton Creek has a 25 m channel width upstream of the Denton Creek Delta. However, when the sand sheets at both locations are scaled to their respective channel width (W_C), they have $6.2* W_C$ vs $5*W_C$ lengths and $4.4*W_C$ vs $5.1*W_C$ widths. This indicates that these sheet deposits scale well to the channel that forms them when comparing two formative channels of different magnitudes.

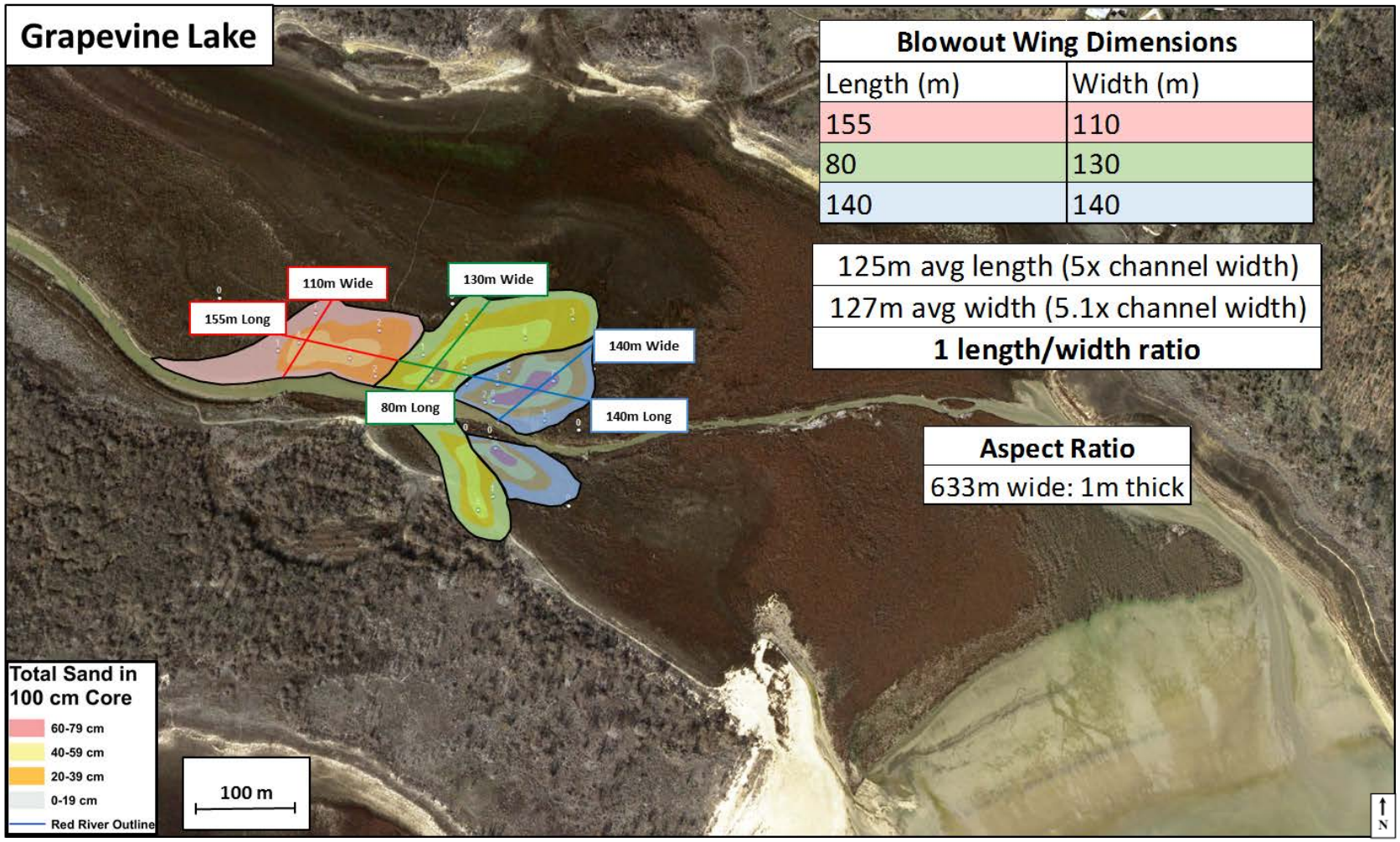

Fig. 35: Grapevine Lake blowout wing dimensions have an average lengths of 125 m and widths of 127 m. They have an average length-to-width ratio of 1.0 and an aspect ratio of 633 (633 m width per 1 m thickness).

Overbank Sand Sheet / Blowout Wing Interpretation

Blowout wings record sand-rich hyperpycnal sheets formed by lateral escape of bedload from the prograding delta channel. Rocks created by turbulent, hyperpycnal underflows, hyperpycnites, have unique sedimentary features (Mulder et al., 2003) that are bore by the blowout wings. Zavala et al. (2006) developed a sedimentary facies model for quasi-steady (long term sustaining flow) hyperpycnites within the lacustrine Rayoso Formation, Argentina (Fig. 36) (Zavala et al., 2006). The model incorporates experimentally confirmed progressions of sedimentary structures that are produced by a waning flow. A decelerating hyperpycnal flow will begin with low-angle cross stratification, transition to parallel lamination, and end with climbing ripples (Simons et al., 1965, Southard, 1991). Zavala et al. (2006) applied this model to the lacustrine hyperpycnites of the Rayoso Formation and determined that additional characteristics of hyperpycnites are a "sharp (non-erosional) base" and potential transition back and forth between sedimentary structures recording fluctuations in the hyperpycnal flow velocity.

In the first phase of the hyperpycnite model, the acceleration phase, the deposit begins on top of prodelta mud and may record deposition of ripples, planar lamination, and low-angle cross beds as the flow ramps up. The second phase, termed the erosion-plus-bypass phase, begins when the flow first passes the erosion threshold for sand and continues through the erosion threshold for consolidated mud; the erosion phase dislodges sand from upstream as well as mud chips if the consolidated mud erosion threshold is surpassed. The erosion phase reportedly may wipe out the deposits created up to that point. Phase three, the deceleration phase, records the deposition of sand and mud chips as they wane through the three sedimentary structures, ending with mud accumulation recording the end of the flow (Zavala et al. 2006). The authors noted

that, depending on the rate of flow deceleration, hyperpycnites may not record the whole suite of sedimentary features from the hyperpycnite model.

The blowout wings from the Red River Delta are a strong modern analogue for the hyperpycnite depositional model described based on the rocks described by Zavala et al, 2006. Each blowout wing contains the corresponding muddy prodelta base, a sharp basal contact, followed by climbing ripple, low-angle cross stratified sand, and a mud cap recording the end of the flow event (Fig. 28). Local mud chips and organic debris record upstream flow acceleration past the erosional threshold for consolidated mud (Fig. 28). Dewatering structures are prevalent at the top of the cores; combined with the wing juxtaposition to the channel and levees, wings record subaerial overbank deposition. The primary difference between our model for blowout wing deposition and Zavala et al (2006) model is that their model is for hyperpycnites flowing into the basin from the channel mouth, and we propose blowout wings are an overbank depositional body recording overspill of the levees.

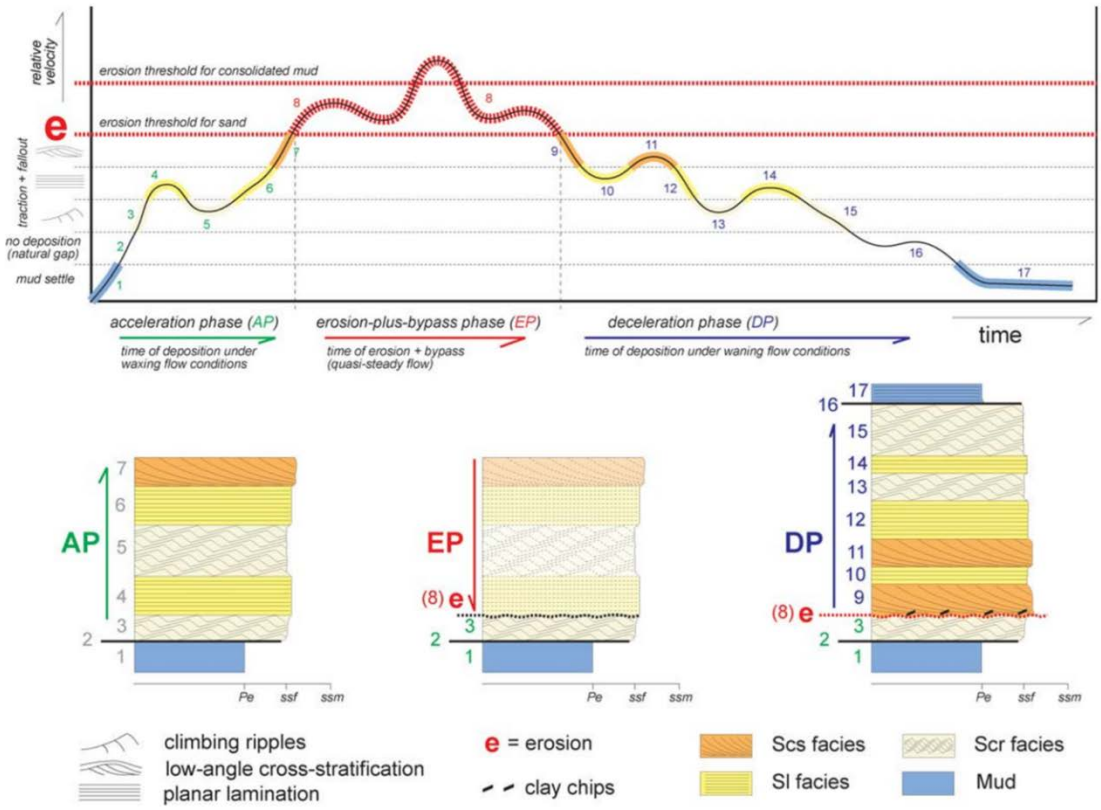

Fig. 36: Hyperpycnite model for turbulent hyperpycnal flows. AP (acceleration phase) deposits are created as flow rises. EP (erosion phase) is defined by the flow velocity passing the erosion threshold for sand and consolidated mud. The DP (deceleration phase) records the deposition of sand and mud chips as they wane through the three sedimentary structures, ending with mud accumulation recording the end of the flow (Zavala et al., 2006).

4.1. Conceptual Model of Delta Formation

The following is a proposed model of formation for the Red River Delta based on the observed architectural element assemblage.

(1) Following an avulsion, breached levees provide a local source of sediment that is redistributed by the newly formed distributive channel as lobate splay deltas.

(2) As the splay delta evolves, the main distributive delta channel lengthens from the avulsion node and begins to segregate suspended load from bedload within the channel. There is a critical point where the channel lengthens sufficiently to fully starve the river mouth of sand. A fully sand starved mouth solely forms a muddy prodelta devoid of delta-front sand that is easily erodible by the channel, positively influencing progradation and extension of the delta channel without bifurcation (Fig. 37). Bifurcation is suppressed due to the complete absence of sand in the mouth to form mouth bars that drive bifurcation of flow. The ever lengthening channel enhances stagnation of upstream bedload sand due to the backwater effect. Bedload sand is stored upstream in the form of mid-channel and side attached bars and the turbulent jet at the river mouth deposits water-saturated mud. Muddy subaqueous levees stabilize over time due to compaction and vegetation; this produces a hardened channel similar to the findings of Hull (2016), who compared resistant clay levees of tie channels to a gun barrel. A lack of sand in the river mouth of non-bifurcating channels is a consistent trend reported for non-bifurcating deltas and tie channels (Rowland et al., 2005; Rowland et al., 2010; Tomanka, 2013; Hull, 2016).

(3) During high-precipitation events (Fig. 38), fluvial discharge into the basin substantially increases (Fig. 39). This increase in flow velocity corresponds to an increased bed shear stress in the delta channel. Sufficiently high velocity flows overcome the erosional threshold of upstream

stored sand bars, flushing them down stream in the channel as a wave of sand. High precipitation events correspond to large surges in Red River discharge, resulting in an increase in discharge to 60,000 ft^3/s or even 175,000 ft^3/s in some cases (Fig. 40).

(4) Levee height decreases basinward. The hardened gun barrel levees are resistant to breakdown by the flow. As the sand wave moves down the delta channel, levees increasingly lose the ability to contain the flow. There is a threshold where the flow of sand becomes higher than the downstream diminishing levees. Sand then tops the levees in a diffusive manner, and is deposited lateral to the channel as thin hyperpycnite sand sheets on top of the levees and into the basin. Decreasing levee height downstream and wings deposited adjacent to the channels have also been documented at the Denton Creek Delta (Tomanka, 2013).

(5) The process of sand blowout removes sand from the channel, reinforcing the dominance of mud at the river mouth. This gives way to continued progradation without bifurcation of the muddy delta channel. The deposits left behind will be splay deltas near the location of avulsion, prodelta muds, channels cutting through the splay delta and prodelta muds, and sand sheets lateral to the channel as wings over older prodelta and levee deposits (Fig. 33).

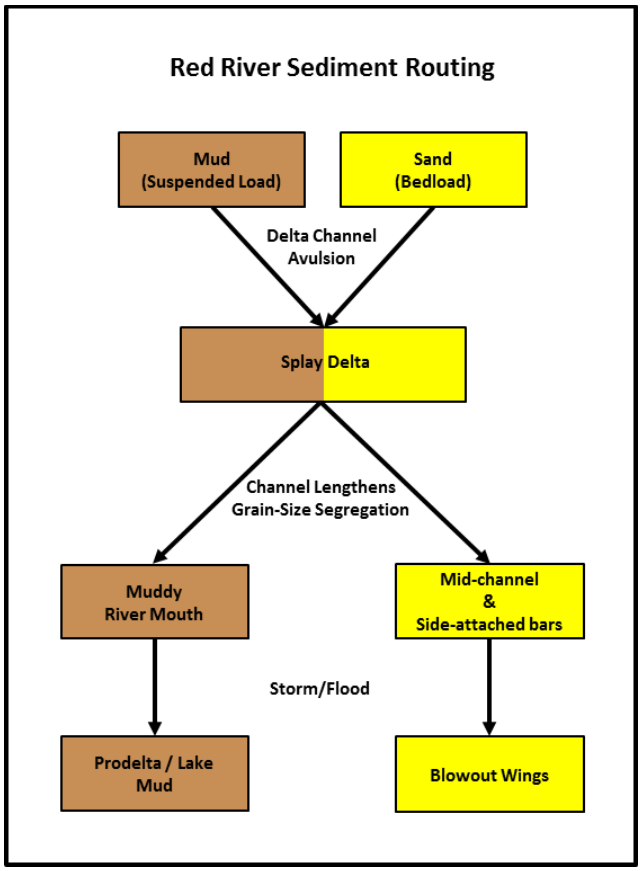

Fig. 37: Sediment routing flow chart for the Red River Delta explaining the depositional relationships between the suspended load and the bedload that produce the interpreted architectural elements.

Fig. 38: Due to the relatively small basin size, Lake Texoma is susceptible to large water level fluctuations. Image taken following a flood in 2015.

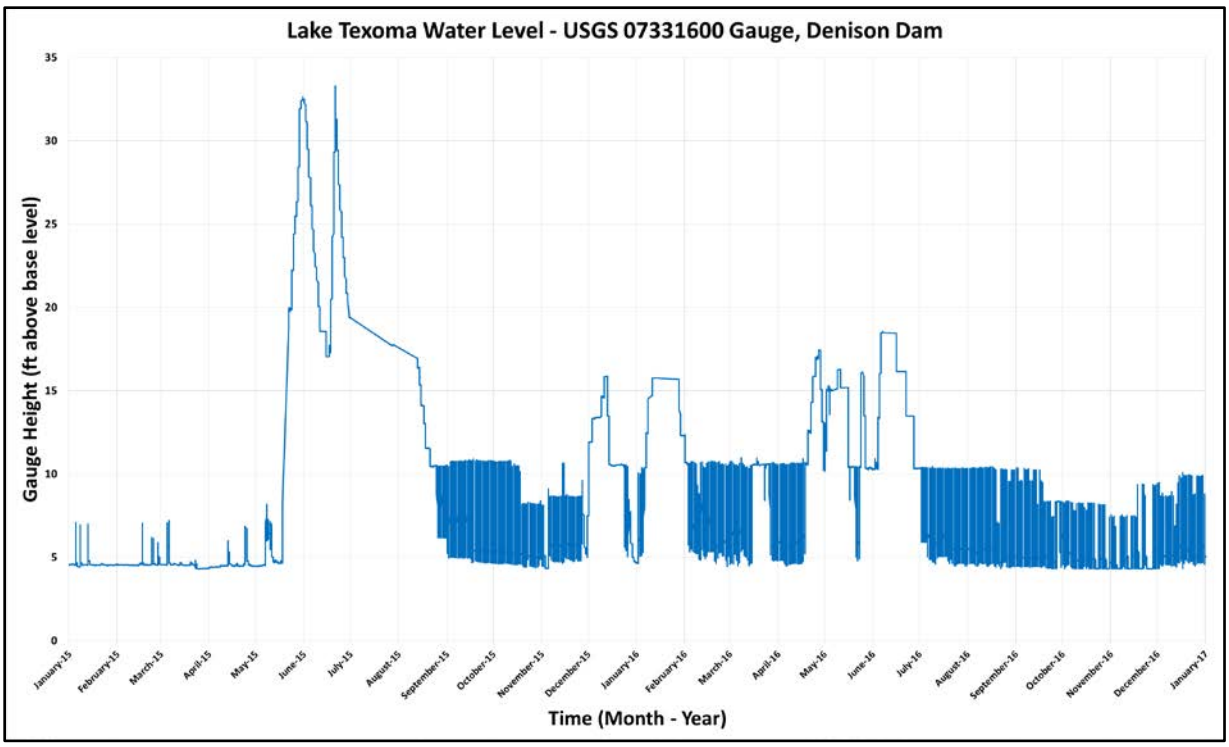

Fig. 39: Lake Texoma water level fluctuation from 2015 to 2017 (USGS, 2017).

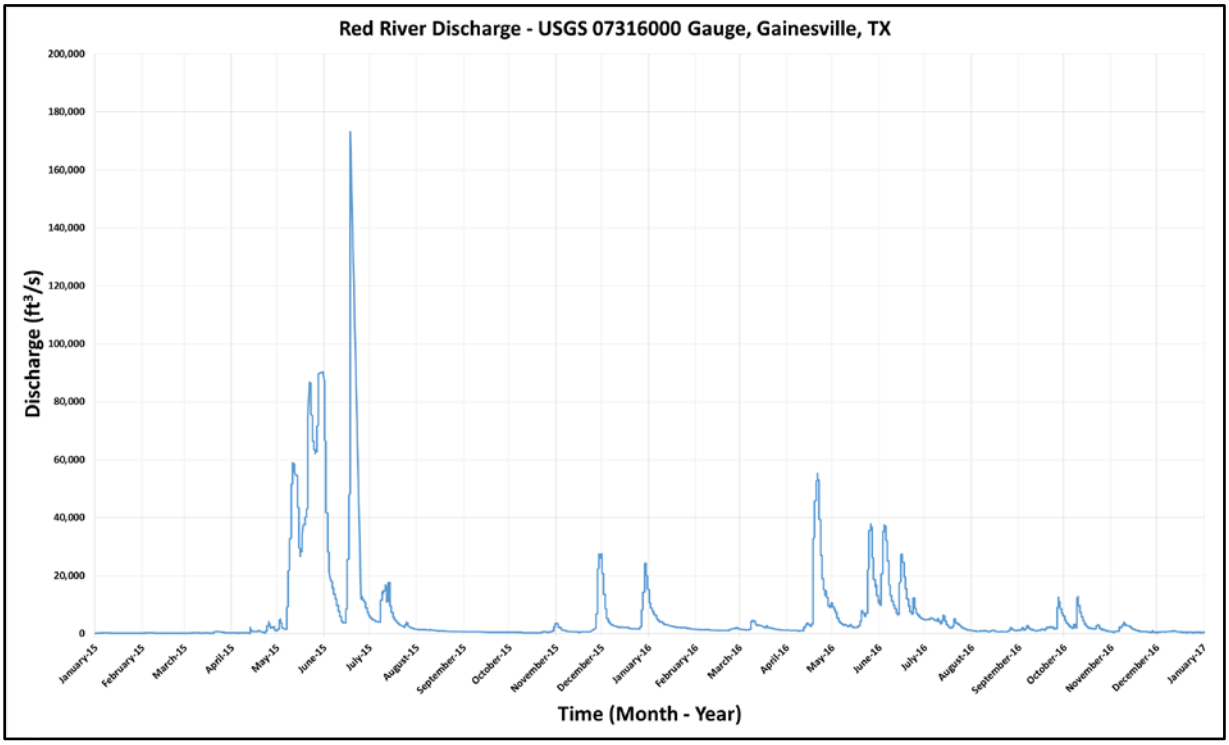

Fig. 40: Red River discharge from 2015 to 2017 (USGS, 2017)

Numerical morphodynamic models that successfully produce elongate, prograding channels always eventually produce mouth bar deposits that lead to bifurcation (Edmonds and Slingerland, 2010; Canestrelli et al., 2014). I propose these models fail to replicate the non-bifurcating morphology characteristic of tie channels and fluvio-deltaic channels due to the incorrect assumption that sand is being incorporated into the turbulent jet that builds single-channel, non-bifurcating deltas. In models, settings for the proportion of fine sediment versus coarse sediment are estimated to be deposited at the river mouth. However, in nature, the Red River Delta and other prograding single-channel deltas show an absence of sand reaching the river mouth (Rowland et al., 2005; Rowland et al., 2010; Tomanka, 2013; Hull, 2016). Future models of non-bifurcating deltas should consider this observed phenomenon.

The backwater effect and the associated process of grain size separation detailed here should be present in the majority of intracratonic basins. The Red River Delta serves as an example of the gun barrel model for delta formation working in a sandy, bed-load dominated river. Tomanka (2013) showed that it works in a muddy, suspended-load dominated river at Grapevine Lake. Hull (2016) displayed its utility for tie channels in the Grijalva River system. Therefore, the gun barrel model is not only a model for fluvio-deltaic channels or tie channels, but is in fact a model for the deposition of the default delta.

Regardless of sand load, the delta front built by mud will always outrun the sand and make a prograding channel “gun barrel” delta. The way you get bifurcation in these muddy lake deltas is to destroy this gun barrel with waves and tides, or clog the barrel with hardened mud or debris that simulate the mouth-bar effect of flow divergence. Lacustrine deltas have weaker basinal forces compared to the wave and tidal energy in oceans, and single-channel, non-bifurcating deltas form in lakes because of this difference. The fluvial energy in the system is

able to control the grain-size of sediment being delivered to the river mouth and in the majority of cases is more dominant than the low basin energy of the lake, leading to the formation of a delta that resembles the morphology of a fluvial channel.

4.4. Importance of blowout wings on subsurface reservoir models

Blowout wings at Lake Texoma and Grapevine Lake emanate and extend laterally from the delta channel axis for 4-6 times the channel width. As the delta channel progrades into the lake basin, these wings form composite sheets that connect up dip fluvial deposits to more basinal rocks. Although individual wings are relatively thin with thicknesses of 10-40cm, they are composed of fine-to-medium grained sand which will have the potential to transmit fluids and gas. Therefore, these wings may serve as vital connectors in reservoirs with analogous environments of deposition. Wings may serve as migration pathways between basinal source rocks and up dip fluvial reservoir rock, or as a complex network of connecting nodes between otherwise isolated reservoir channel bodies, resulting in higher total reservoir volume.

This work serves as the first to quantify the dimensions of blowout wings and scale them to the formative channel width (Fig. 34, 35). Their aspect ratios may serve useful for extending 2D log data (thickness) of wings into the lateral dimension. Wings in core, such as those pictured from the Mungaroo formation (Fig. 41) would traditionally be ignored as reservoir contribution. Perforating thin, sandy blowout wings as these in addition to the main reservoir may increase overall reserves.

Fig. 41: Noblige-2 core of the Mungaroo Formation, Western Australia. These thin sands may be blowout wings and have the potential to improve reservoir connectivity.

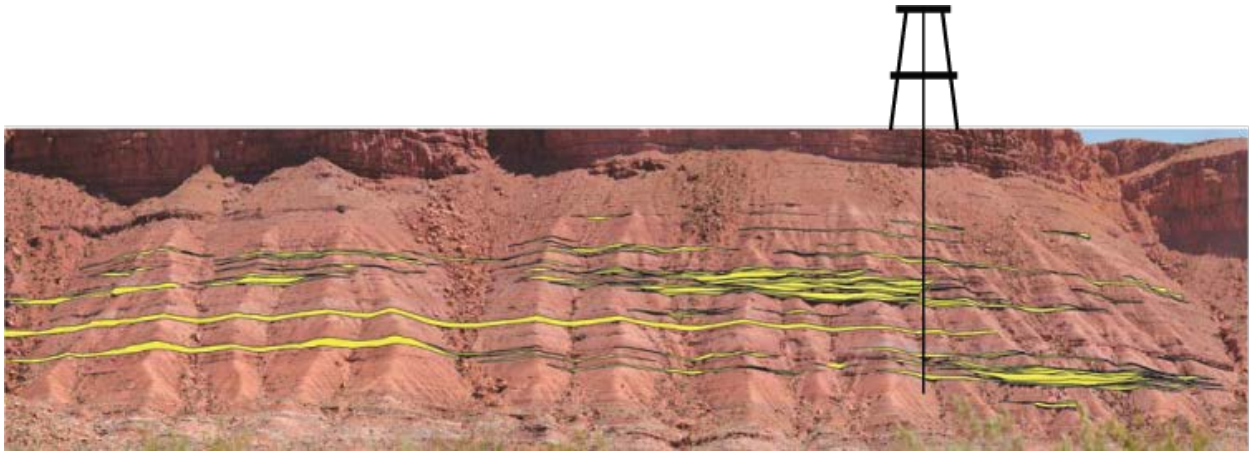

Fig. 42: Kayenta Formation, Warner Valley, UT outcrop showing interpreted channels connected by thin, laterally continuous wings. Oil derrick drawn in to depict the potential of wings to connect otherwise isolated sands to one wellbore (modified from Huling and Holbrook, 2016).

In a study on the Kayenta Formation in Warner Valley, Utah, Huling and Holbrook (2016) demonstrated the statistical clustering of elongate muddy delta lobes (Fig. 42). They note the similarity between the ancient Kayenta Formation and the modern fluvio-deltaic environment of Grapevine Lake. The Kayenta primarily consists of a matrix of lacustrine mud and fine sediment with sandy deltaic channels recording linear propagation as ribbons. The sandy fluvio-

deltaic channel fills notably had thin sand sheets they interpreted as blowout wings that extended laterally from the channel. High-accommodation fluvial systems have been shown to cluster due to non-random stream avulsion centered on a primary channel axis (Hull and Holbrook, 2016). The recognition of blowout wings greatly increases the potential static connectivity of fluvial bodies by connecting otherwise isolated channels through a network of laterally extensive wings. Adding blowout wings into the lexicon of high-accommodation fluvial depositional models should be considered for subsurface exploration.

CHAPTER 5 – CONCLUSIONS

(1) Field mapping of sediment distribution at the Red River Delta, Lake Texoma shows that even in a bedload-dominated, sandy river system, sand does not reach the river mouth and forms a muddy, non-bifurcating delta. This phenomenon is due to a process of grain size segregation when the channel has sufficient length to separate the bedload sand and the suspended load clay. Given enough channel length, mud and sand dominated river systems will form non-bifurcating, single-channel deltas. Therefore, this is the default delta.

(2) During high discharge flow events, sand stored upstream as mid-channel and side-attached bars are transported downstream and deposited into the basin as overbank sand sheets called blowout wings.

(3) The architectural elements left in the rock record for a single-channel lacustrine delta will be prodelta muds, splay deltas, channel fills, and sandy blowout wings.

(4) Blowout wings are a modern example of a hyperpycnite as described by Zavala (2006).

(5) Blowout wings have aspect ratios of up to 2,480 m wide per 1 m thick. In this study they have an average thickness of 26 cm. Their dimensions scale to the formative channel width (W_C). They have lengths of $5.75*W_C$ and widths of $4.75*W_C$.

(6) Blowout wings are potential sources of connectivity within high-accommodation fluvial reservoirs. Therefore, they may be useful for petroleum exploration of subsurface reservoirs.

(7) Blowout wings serve as an extension of the fluvio-deltaic architectural element lexicon, and should be considered when interpreting high-accommodation fluvial environments of deposition.

REFERENCES

Abramovich, G. N. (1963), Theory of Turbulent Jets, MIT Press, Cambridge, Mass.

Albertson, M. L., Y. B. Dai, R. A. Jensen, and H. Rouse (1950), Diffusion of submerged jets, Trans. Am. Soc. Civil Eng., 115, 639–664.

Ashton, A. D., and L. Giosan (2011), Wave-angle control of delta evolution, Geophys. Res. Lett., 38, L13405, doi:10.1029/2011GL047630.

Bates, C. C. (1953), Rational theory of delta formation, AAPG Bull., 37(9), 2119–2162

Bhattacharya, J. P., and L. Giosan (2003), Wave-influenced deltas: Geomorphological implications for facies reconstruction, Sedimentology, 50, 187–210.

Blake, D. H., and C. D. Ollier (1971), Alluvial plains of the Fly River, Papua, Z. Geomorphol., 12, Suppl., 1–17.

Boggs, S (1995), Principles of Sedimentology and Stratigraphy, Prentice Hall Publishing Company.

Caldwell, R. L. (2013), The effect of grain size on river delta process and morphology, M.S. thesis, 72 pp., Boston College, Boston, Massachusetts.

Caldwell, R. L., and D. A. Edmonds (2014), The effects of sediment properties on deltaic processes and morphologies: A numerical modeling study, J. Geophys. Res. Earth Surf., 119, 961–982

Canestrelli, A., W. Nardin, D. Edmonds, S. Fagherazzi, and R. Slingerland (2014), Importance of frictional effects and jet instability on the morphodynamics of river mouth bars and levees, J. Geophys. Res. Oceans, 119, 509–522, doi:10.1002/2013JC009312.

Celoria, F., (1996), Delta as a Geographical Concept in Greek Literature. Isis Vol. 57, No. 3, pp. 385-388.

Dalrymple, R. W., and K. Choi (2007), Morphologic and facies trends through the fluvial–marine transition in tide-dominated depositional systems: A schematic framework for environmental and sequence-stratigraphic interpretation, Earth Sci. Rev., 81(3–4), 135–174.

Day, G., W. E. Dietrich, J. C. Rowland, and A. Marshall (2008), The depositional web on the floodplain of the Fly River, Papua New Guinea, J. Geophys. Res., 113, F01S02, doi:10.1029/2006JF000622.

Edmonds, D. A., and R. L. Slingerland (2007), Mechanics of river mouth bar formation: Implications for the morphodynamics of delta distributary networks, J. Geophys. Res., 112, F02034, doi:10.1029/2006JF000574.

Edmonds, D. A., and R. L. Slingerland (2010), Significant effect of sediment cohesion on delta morphology, Nat. Geosci., 3(2), 105–109.

Ertel, H. (1942), Einneuerhydrodynamischer Wirbelsatz, Meteorol. Z., 59(2), 277–281.

Esposito, C. R., I. Y. Georgiou, and A. S. Kolker (2013), Hydrodynamic and geomorphic controls on mouth bar evolution, Geophys. Res. Lett., 40, 1540–1545, doi:10.1002/grl.50333.

ESRI (2017). ArcGIS Desktop Release 10.4. Redlands, CA: Environmental Systems Research Institute.

Fagherazzi, S. (2008), Self-organization of tidal deltas, Proceedings of the National Academy of Sciences of the United States of America, 105(48), 18692-18695.

Fagherazzi, S., and I. Overeem(2007), Models of deltaic and inner continental shelf landform evolution, Annu. Rev. Earth Planet. Sci., 35, 685–715.

Fagherazzi, S., D. A. Edmonds, W. Nardin,N. Leonardi, A. Canestrelli, F. Falcini, D. J. Jerolmack, G. Mariotti, J. C. Rowland, and R. L. Slingerland (2015), Dynamics of river mouth deposits, Rev. Geophys., 53, 642–672, doi:10.1002/2014RG000451.

Falcini, F., and D. J. Jerolmack (2010), A potential vorticity theory for the formation of elongate channels in river deltas and lakes, J. Geophys. Res., 115, F04038, doi:10.1029/2010JF001802.

Galloway, W. E. (1975), Process framework for describing the morphologic and stratigraphic evolution of deltaic depositional systems, in Deltas: Models for Exploration, edited by M. L. Broussard, pp. 87–98, Houston Geol. Soc., Houston, Tex.

Google Earth (2017). Website. https://www.google.com/earth/.

Hoyal, D. C. J. D. et al. (2003), Sedimentation from Jets: A Depositional Model for Clastic Deposits of all Scales and Environments, Salt Lake City: ExxonMobile.

Huling, G. and Holbrook, J. (2016), Clustering of elongate muddy delta lobes within fluvio-lacustrine systems, Jurassic Kayenta Formation, Utah, in Budd, D.A., Hajek, E.A., and Purkis, S.J. (eds.), Autogenic Dynamics and Self-Organization in Sedimentary Systems: SEPM Special Publication 106, 18p.

Hull, M. (2016), A modern reservoir analogue for a poorly drained “high accommodation” fluvial system: Sedimentary processes, architecture, and reservoir connectivity of the Grijalva system, Tabasco State, Mexico, Ph.D. thesis, 139 pp., The University of Texas at Arlington, Arlington, Texas.

Jerolmack, D. J., and J. Swenson (2007), Scaling relationships and evolution of distributary networks on wave-influenced deltas, Geophys. Res. Lett., 34, L23402, doi:10.1029/2007GL031823.

Jirka, G. H. (1994), Shallow jets, in Recent Research Advances in the Fluid Mechanics of Turbulent Jets and Plumes, edited by P. A. Davies and M. J. Valente Neves, pp. 155–175, Kluwer Acad., Dordrecht, Netherlands.

Leonardi, N., A. Canestrelli, T. Sun, and S. Fagherazzi (2013), Effect of tides on mouth bar morphology and hydrodynamics, J. Geophys. Res. Oceans, 118, 4169–4183, doi:10.1002/jgrc.20302.

Nardin, W., and S. Fagherazzi (2012), The effect of wind waves on the development of river mouth bars, Geophys. Res. Lett., 39, L12607, doi:10.1029/2012GL051788.

Nardin, W., G. Mariotti, D. A. Edmonds, R. Guercio, and S. Fagherazzi (2013), Growth of river mouth bars in sheltered bays in the presence of frontal waves, J. Geophys. Res. Earth Surf., 118, 872–886, doi:10.1002/jgrf.20057.

NASA (2016). Website, http://visibleearth.nasa.gov/view.php?id=8103.

Olariu, C., J. Bhattacharya, M. Leybourne, S. Boss, and S. Stern (2012), Interplay between river discharge and topography of the basin floor in a hyperpycnal lacustrine delta, Sedimentology, 59 (2), 704-728, doi: 10.1111/j.1365-3091.2011.01272.

Orton, G. J., and H. G. Reading (1993), Variability of deltaic processes in terms of sediment supply, with particular emphasis on grain size, Sedimentology, 40, 475–512.

Overeem, I., J. P. M. Syvitski, and E. W. H. Hutton (2005), Three-dimensional numerical modeling of deltas, in River Deltas: Concepts, Models and Examples, SEPM Spec. Publ., edited by J. P. Bhattacharya and L. Giosan, 83 pp., 13–30, SEPM, Tulsa, Okla.

Ozsoy, E., and U. Unluata (1982), Ebb-tidal flow characteristics near inlets, Estuarine Coastal Shelf Sci., 14(3), 251–263.

Postma, G. (1990), Depositional architecture and facies of river and fan deltas; a synthesis, *Special Publication of the International Association of Sedimentologists, 10, 13-27.*

Rowland, J. C., M. T. Stacey, and W. E. Dietrich (2009a), Turbulent characteristics of a shallow wall-bounded plane jet: Experimental implications for river mouth hydrodynamics, J. Fluid Mech., 627, 423–449, doi:10.1017/S0022112009006107.

Rowland, J. C., W. E. Dietrich, G. Day, and G. Parker (2009b), Formation and maintenance of single-thread tie channels entering floodplain lakes: Observations from three diverse river systems, J. Geophys. Res., 114, F02013, doi:10.1029/2008JF001073.

Rowland, J. C. (2007), Tie channels, Ph.D. thesis, 176 pp., Univ. of California, Berkeley, Calif.

Rowland, J. C., W. E. Dietrich, and M. T. Stacey (2010), Morphodynamics of subaqueous levee formation: Insights into river mouth morphologies arising from experiments, J. Geophys. Res., 115, F04007, doi:10.1029/2010JF001684.

Schwartz, D (1978), Sedimentary Facies, Structures, and Grain Distribution: The Red River in Oklahoma and Texas. Gulf Coast Association of Geological Societies Transactions Vol. 28, Pages 473-492.

Simons, D.B., E.V. Richardson, and C.F. Nordin (1965), Sedimentary structures generated by flow on alluvial channels, in Middleton, G.V., ed., Primary Sedimentary Structures and Their Hydrodynamic Interpretation: Society of Economic Paleontologists and Mineralogists, Special Publication 12, p. 34–52.

Southard, J.B. (1991), Experimental determination of bedform stability: Annual Review of Earth and Planetary Sciences, v. 19, p. 423–455.

Syvitski, J. P. M., and Y. Saito (2007), Morphodynamics of deltas under the influence of humans, Global Planet. Change, 57(3–4), 261–282.

Tennekes, H., and J. L. Lumley (1972), A First Course in Turbulence, 300 pp., MIT press, Cambridge Mass.

Thien, S. (1979). A Flow Diagram for Teaching Texture-by-feel Analysis. Journal of Agronomic Education. Volume 8, pp. 54-55.

Texas Natural Resources Information Systems (2017). Website. https://tnris.org/.

Texas Water Development Board (1967). http://www.fwspubs.org/doi/suppl/10.3996/012015-JFWM-003/suppl_file/012015-jfwm-003.s2.pdf?code=ufws-site.

Texas Water Development Board (2002). http://www.twdb.texas.gov/surfacewater/surveys/completed/files/Texoma/2002-07/Texoma2002_FinalReport.pdf.

Texas Water Development Board (2011). http://www.twdb.texas.gov/surfacewater/surveys/completed/files/Grapevine/2011-09/Grapevine2011_FinalReport.pdf.

Tomanka, G. (2013). Morphology, Mechanisms, and Processes for the Formation of a Non-bifurcating Fluvial-Deltaic Channel Prograding into Grapevine Reservoir, Texas. Master's Thesis, Texas Christian University.

Wright, L. D. (1977), Sediment transport and deposition at river mouths: A synthesis, Geol. Soc. Am. Bull., 88(6), 857–868.

Wright, L.D. and Coleman, J.M. (1973) Variations in morphology of major river deltas as functions of ocean wave and river discharge regimes. AAPG Bull., 57, 370–398.

Zavala, C., J. Ponce, M. Arcuri, D. Drittanti, H. Freije, and M. Asensio (2006), Ancient Lacustrine Hyperpycnites: A Depositional Model from a Case Study in the Rayoso Formation (Cretaceous) of West-Central Argentina. J Sediment Res 76, 41–59. doi:10.2110/jsr.2006.

VITA

Tyler Howe was born January 8, 1992 and grew up in Norman, Oklahoma. He is the son of Todd and Tracy Howe. A 2010 graduate of Norman High School, he earned his Bachelor of Science with a major in Petroleum Geology and a minor in Philosophy from the University of Oklahoma in 2015.

He lives in Dallas, Texas with his fiancé, Sheena, and his sheepdog Hank. Following graduation, he will be joining Pioneer Natural Resources working as a geologist.

ABSTRACT

THE EVOLUTION AND STRATIGRAPHIC ARCHITECTURE OF FLUVIO-LACUSTRINE DELTAS: RESERVOIR CHARACTERISTICS FROM THE RED RIVER DELTA, LAKE TEXOMA AND THE DENTON CREEK DELTA, GRAPEVINE LAKE, TX

Tyler Howe, M.S., 2017
Department of Geology
Texas Christian University

Dr. John Holbrook, Thesis Advisor, Professor of Geology
Dr. Michael Slattery, Professor of Geology
Tamie Morgan, Professor of Professional Practice

Elongate, single-channel, non-bifurcating deltas are currently forming in many lakes throughout the United States. The Red River Delta forms an elongate, single-delta into Lake Texoma, sourced by a sand-rich, bedload dominated river system. Current models of delta formation suggest muddy rivers can form elongate deltas due to a lack of sand to form mouth bars, driving bifurcation, but do not explain a mechanism for a sandy river to form a non-bifurcating delta. We propose a model for elongate, single-channel deltas based on a process of grain-size separation within the delta channel, resulting in a sand starved river mouth that cannot bifurcate. Our results indicate that elongate, non-bifurcating deltas should be formed by muddy and sandy rivers alike, and therefore may represent the default delta. Field mapping at Lake Texoma and Grapevine Lake show that these single-channel deltas are found to be associated with overbank sand sheets that emanate laterally from the channel axis. These wings are interpreted to be blowout wings (after Tomanka, 2013) and are a modern example of lacustrine

hyperpycnites (after Zavala, 2006). These wings are thin (10-40cm) and laterally continuous, with lengths and widths spanning several hundred meters from the channel, and aspect ratios reaching 2,480m wide per 1m thickness. Blowout wings are found to scale to the formative depositional system, with dimensions corresponding to 5x the channel width. The recognition of blowout wings greatly increases the potential static connectivity of fluvial bodies by connecting otherwise isolated channels through a network of laterally extensive wings. Adding blowout wings into the lexicon of high-accommodation fluvial depositional models should be considered for subsurface exploration.